Decoding the Variant-to-Function Relationship for *LIPA*, a Risk Locus for CAD

Fang Li,[1*] Elise Flynn,[2,3] Jianting Shi,[1] Xun Wu,[1] Ziyi Wang,[1] Chenyi Xue,[1] Haoxiang Cheng,[4] Yujiao Meng,[1] Jian Cui,[1] Yizhou Zhu,[5] Annie Rozenblyum,[1] Jeana Chun,[1] Antonio Hernandez-Ono,[6] Babak Razani,[7] Marit Westerterp,[8] Robert C Bauer,[1] Yousin Suh,[5] Ke Hao,[4] Tuuli Lappalainen,[2,3] Hanrui Zhang[1*]

1. Cardiometabolic Genomics Program, Division of Cardiology, Department of Medicine, Columbia University Irving Medical Center, New York, NY, USA
2. New York Genome Center, New York, NY, USA
3. Department of Systems Biology at Columbia University, New York, NY, USA
4. Department of Genetic and Genomic Sciences, Icahn School of Medicine at Mount Sinai, New York, NY, USA
5. Department of Obstetrics and Gynecology, Department of Genetics and Development, Columbia University Irving Medical Center, New York, NY, USA
6. Department of Medicine, Vagelos College of Physicians and Surgeons, Columbia University, New York, NY, USA
7. Division of Cardiology and Vascular Medicine Institute, the Department of Medicine, and the Department of Veterans Affairs, University of Pittsburgh, Pittsburgh, PA, USA
8. Department of Pediatrics, University Medical Center Groningen, University of Groningen, Groningen, The Netherlands

*** Corresponding authors:**
Fang Li PhD
Cardiometabolic Genomics Program,
Division of Cardiology, Department of Medicine
Columbia University Irving Medical Center
630 West 168th Street, P&S10-401
New York, NY 10032
Tel: (212) 305-3508
Email: fl2532@cumc.columbia.edu

Hanrui Zhang PhD
Cardiometabolic Genomics Program,
Division of Cardiology, Department of Medicine
Columbia University Irving Medical Center
630 West 168th Street, P&S10-401
New York, NY 10032
Tel: (212) 304-7905
Email: hz2418@cumc.columbia.edu

Key Words: Atherosclerosis, Functional Genomics, GWAS, Lysosomal Acid Lipase, Macrophage

NONSTANDAR ABBREVIATIONS AND ACRONYMS

BMDM, bone marrow-derived macrophage
CAD, coronary artery disease
CESD, cholesterol ester storage disease
eQTL, expression quantitative trait loci
GTEx, Genotype-Tissue Expression Portal
GWAS, genome-wide association study
HMDM, human monocyte-derived macrophage
HDL, high-density lipoprotein
IPA, ingenuity pathway analysis
LIPA, lysosomal acid lipase
LD, linkage disequilibrium
LDL, low-density lipoprotein
PM, peritoneal macrophage
SNP, single-nucleotide polymorphism
STARNET, Stockholm-Tartu Atherosclerosis Reverse Networks Engineering Task study

CLINICAL PERSPECTIVE

What is New?

- CAD GWAS variants at the *LIPA* locus led to increased macrophage LIPA expression and enzyme activity.
- Myeloid-specific overexpression of *Lipa* exacerbates atherosclerosis.
- Our study connected the genetic variation to the involved cell type and the target gene, and the disease mechanism for this important locus.

What are the Clinical Implications?

- GWAS and meta-analyses have identified over 200 loci for CAD. Establishing the candidate genes and their mechanistic studies inform novel biological mechanisms and therapeutic application.
- There is strong statistical evidence linking *LIPA* with CAD. By leveraging functional genomic studies and transgenic mice, our work established the direct causality that *LIPA* risk alleles drive increased myeloid LIPA and aggravate atherosclerosis. Establishing the variant-to-function relationship for this locus informs that increasing myeloid LIPA may not be a therapeutic strategy for CAD, despite the essential role of LIPA in regulating lysosomal lipid metabolism.

ABSTRACT

Background: Genome-wide association studies revealed a robust association between genetic variants in the *LIPA* (lysosomal acid lipase) gene and coronary artery diseases (CAD), but not lipid traits. QTL studies support that the risk alleles of *LIPA* CAD variants are associated with higher *LIPA* mRNA and enzyme activity in human monocytes. Yet the variant-to-function relationship and how this important locus impacts disease etiology has not been fully established. Herein, we aim to determine the causal variant(s), involved cell type, and the target gene, establish the causality of the variant-to-function relationship, and elucidate how increased myeloid LIPA impacts atherosclerosis *in vivo*.

Methods: We apply functional genomic datasets, post-GWAS prioritization pipelines, and molecular biology techniques, incuding eQTL, enzyme activity-QTL, high-resolution Tri-HiC, ChIP-seq, and site-directed mutagenesis and luciferase assay to connect functional variants to the candidate genes in the causal cell type. To establish how increased myeloid *LIPA* impacts atherosclerosis, we generated myeloid-specific *Lipa* overexpression mice (*Lipa*^{Tg}).

Results: Post-GWAS pipelines support *LIPA* as the candidate causal gene at the locus. In human monocyte-derived macrophages, *LIPA* mRNA, protein and enzyme activity were higher in the risk allele carriers of CAD variants. High-resolution Tri-HiC and luciferase assay confirmed an intronic enhancer region showing strong interaction with the *LIPA* promoter. Within the enhancer region, the risk alleles of rs1412444/rs1412445 and rs1320496 demonstrate enhanced binding to PU. 1, and acted as the functional variants with risk alleles leading to increased enhancer activity. The risk allele of rs1320496 is predicted to create a motif binding site for PU.1. The functional genomic data together support that *LIPA* is the candidate causal gene in the locus, and the risk alleles of CAD led to increased LIPA in a myeloid cell-specific manner. Consistently, mice with myeloid-specific *Lipa* overexpression on a *Ldlr*$^{-/-}$ background showed significantly increased atherosclerotic lesion size and lesion macrophage area without affecting plasma cholesterol. ScRNA-seq analysis showed that *Lipa*^{Tg} led to reduced lipid-enriched yet increased inflammatory macrophage subsets, and activation chemokine signaling pathway. This was further confirmed by reduced neutral lipid accumulation in both plaque and peritoneal macrophages and significantly increased monocytes infiltration into the lesion in *Lipa*^{Tg} mice.

Conclusions: We established that *LIPA* risk alleles drive increased myeloid LIPA and aggravate atherosclerosis.

INTRODUCTION

Coronary artery disease (CAD) remains the leading cause of death worldwide. Heritability of CAD has been estimated to be 40% to 60%, supporting the contribution of inherited genetic variation to the its pathogenesis.[1] Genome-wide association studies (GWAS) determine the common genetic variants associated with diseases and traits, and have collectively identified more than 200 CAD-associated risk loci.[2-5] Identifying the causal genes that connecting genetic variation to disease risk will inform novel biological mechanisms and therapeutic targets for CAD.

The *LIPA* locus has been repeatedly identified as a risk locus for CAD in multiple GWAS and meta-analyses (**Supplemental Table I**),[2-12] but not plasma lipid traits,[13] supporting a CAD-specific yet lipid metabolism-independent contribution. Colocalization analysis supports that genetic variants associated with CAD are also associated with *LIPA* expression in the Stockholm-Tartu Atherosclerosis Reverse Networks Engineering Task study (STARNET) datasets,[14] suggesting *LIPA* as the candidate causal gene at the locus. The *LIPA* gene encodes lysosomal acid lipase (also known as LAL), the only known acidic lipase hydrolyzing cholesteryl ester and triglycerides delivered to the lysosome via the uptake of lipoproteins.[15, 16] Rare coding and splicing junction mutations in *LIPA* result in Mendelian disorders, including the infant-onset Wolman Disease due to a complete loss of LIPA and the adult-onset Cholesteryl Ester Storage Disease (CESD) owing to 3-5% residual enzyme activity.[15] CESD is characterized by hepatomegaly, hepatosplenomegaly, and premature atherosclerosis, presumably due to severe dyslipidiemia.[17, 18] Because the lead SNP (single nucleotide polymorphism) for CAD at the *LIPA* locus, rs1412444, is intronic, identifying the functional effects of the non-coding variation on *LIPA* expression is a major challenge.

rs1412444, and other SNPs in high linkage disequilibrium (LD) with rs1412444, showed robust expression quantitative trait locus (eQTL) signals in monocytes, with risk alleles of CAD linked to higher *LIPA* mRNA in human monocytes.[7] Importantly, *LIPA* risk alleles were associated with higher *LIPA* mRNA as well as enzyme activity in human monocytes.[19] These eQTL and enzyme activity QTL analyses support that CAD risk alleles are associated with higher LIPA and monocyte may be causally involved. Pathologically, monocytes play essential roles in the development and exacerbation of atherosclerosis.[20] In atherosclerosis, plaque macrophages are largely derived from circulating monocytes infiltrating the plaque.[21] Monocytes and macrophages may therefore represent the most relevant cell types for the regulatory effects of CAD LIPA variants.

Despite strong statistical association and initial QTL studies supporting the directionality and the potential causal cell types, the variant-to-function relationship and how this important locus impacts atherosclerosis are unclear. Herein, we sought to delineate the causal variants, cell types involved and the effector genes, and the regulatory mechanisms; and determine how LIPA might contribute to atherosclerosis.

METHODS

A detailed description of methods and materials are provided in the Supplemental Materials for the following techniques: human monocyte isolation and monocyte-derived macrophage differentiation, Western Blot, LIPA enzyme activity assay, high-resolution Tri-HiC, plasmid construction and site-directed mutagenesis for luciferase assay, histological analysis of atherosclerosis lesion, monocyte infiltration assay, immunofluorescence staining (IF), plasma lipid measurement, fast protein liquid chromatography (FPLC), culture of murine bone-marrow derived macrophages (BMDM) and peritoneal macrophages (PM), quantitative reverse-transcription polymerase chain reaction (qPCR); modified low-density lipoprotein (LDL) uptake and neutral lipid accumulation, single-cell preparation of mouse aorticspecimens and single-cell RNA sequencing (scRNA-seq), microscopy imaging and quantification. Functional genomic data analyses for colocalization, genotype calling and imputation, post-GWAS prioritization, high-resolution Tri-HiC, and motif and allelic-specific binding analysis, and scRNA-seq data analysis and IPA (Ingenuity Pathway Analysis), are also provided in the Supplemental Materials. All human protocols for this work were approved by the Human Subjects Research Institutional Review Board at Columbia University.

GWAS, eQTL, and Functional Genomic Datasets

The functional genomic analysis incorporated two data sources: GWAS summary statistics from the UK BioBank (UKBB) or Coronary Artery Disease Genome Wide Replication and Meta-analysis plus The Coronary Artery Disease Genetics (CARDIoGRAMplusC4D)[3] and tissue/cell-type specific eQTLs from the Genotype-Tissue Expression project (GTEx) v8,[22] STARNET,[14] or BLUEPRINT.[23]

Transgenic Mouse Model

Mouse model for transgenic overexpression of *Lipa* (*Lipa*$^{fl/wt}$) on C57BL/6 background was generated by embryonic stem cell-based gene targeting by the Genetically Modified Mouse Models Shared Resources at the Columbia University Irving Medical Center. Briefly, *Lipa* open reading frame (NM_001111100) was cloned into the *AscI* site of the backbone vector (Addgene, #74285)[24] for the final construct: homologous left arm-CAG-loxP-STOP-loxP-Lipa-IRES-eGFP-homologous right arm. The inserted segment at the *Rosa26* locus was confirmed by Sanger sequencing.

Atherosclerosis Study

All animal experiments were approved by the Institutional Animal Care and Use Committee at Columbia University. Mice used in this study were on a C57BL/6 background, and age- and sex- matched. *LysMCre*$^{+/+}$ mice (No. 004781) and *Ldlr*$^{-/-}$ mice (No. 002207) were obtained from the Jackson Laboratory. Mice for myeloid-specific overexpression of *Lipa* on an atherosclerosis-prone *Ldlr*$^{-/-}$ background are *LysMCre*$^{+/-}$, *Lipa*$^{fl/wt}$, *Ldlr*$^{-/-}$, referred as *Lipa*^{Tg}, hereinafter. Their littermates, *LysMCre*$^{-/-}$, *Lipa*$^{fl/wt}$, *Ldlr*$^{-/-}$ are used as controls (*Ctl*). Both male and female mice were used and fed with a Western Diet (WD, TD88137, Envigo Teklad) for 16 weeks in atherosclerosis study.

Data and Code Availability

The datasets generated during the current study, including scRNA-seq, will be deposited in the Gene Expression Omnibus (GEO) upon publication. The human macrophage RNA-seq dataset was previously published and is available at DRYAD with identifier doi:10.5061/dryad.866t1g1nb. All code for data

analysis associated with the current submission will be available at https://github.com/hanruizhang/ upon acceptance of the manuscript. Any updates will also be available via the above GitHub repoitory.

Statistical Analysis

All statistical analyses were performed using GraphPad prism 9. When sample size (n) > 6, data were tested for normality using a Shapiro-Wilk test (when n < 8) or D'Agostino-Pearson test (when n ≥ 8). F-test of equality of variances was performed to compare the two sample variances. Data that passed normality tests were presented as mean ± standard error of mean (SEM) and analyzed using two-tailed Student's t-test for comparison of two groups and equal variances (or with Welch's correction if F-test was not satisfied), or one-way ANOVA for one independent variable with more than two groups. Tukey's post-hoc correction for multiple comparisons was applied where appropriate. Data that were not normally distributed were analyzed using nonparametric tests, i.e. Mann-Whitney U test or Kruskal-Wallis test, were presented as median ± 95% confidence interval. Nonparametric tests were also used when n ≤ 5. $P < 0.05$ was considered statistically significant. The number of independent experiments and biological replicates were specified in figure legends for each assay.

RESULTS

Integrative genomic analyses support *LIPA* as the candidate causal gene at the *LIPA* locus, a risk locus for CAD

GWAS have identified a number of common genetic variants at the *LIPA* locus that strongly associate with CAD risks as summarized in **Supplemental Table I**. Three large cohorts, including more than 87,000 cases and 146,000 controls in total, identified three CAD GWAS SNPs (rs1412444, $P = 2.76\times10^{-13}$; rs2246833, $P = 4.35\times10^{-8}$; and rs2246942, $P = 4.3\times10^{-9}$) reside in the intronic region of the *LIPA* gene in European and South Asian populations (**Figure 1A** and **Supplemental Table I**).[6-8]

To nominate the causal gene at the locus, we applied integrative genomic analyses (IGA) pipelines leveraging GWAS and eQTL datasets for statistical inference.[25] The IGA pipeline incorporated two broad methods, including colocalization analysis and Summarized Mendelian Randomization (SMR). Colocalization analysis assesses the posterior probability that GWAS CAD statistics and eQTL datasets share the same causal variant(s).[26] Using CARDIoGRAMplusC4D GWAS and GTEx eQTL datasets, our analysis revealed that *LIPA* is the only nearby gene showing strong regional colocalization probability (rcp = 0.66) in this region (1Mb flaking gene *LIPA*) (**Figure 1B** and **Figure IA**). By integrating STARNET (an eQTL dataset in disease-relevant tissues collected from ~600 CAD patients) with GWAS summary statistics in this region (500 kb flanking gene *LIPA*), we confirmed that *LIPA*, but not other nearby genes, showed significant colocalization signal (Coloc $H_4 > 0.8$) in the diseased tissues (**Supplemental Table II**), further supporting *LIPA* as the candidate causal gene. SMR differentiated the genuine causal gene (the same variants associated with the gene expression and traits due to causality or pleiotropy) from genes whose expression associated with complex traits because of the LD between independent causal variants.[27, 28] We applied SMR on GWAS summary statistics and STARNET datasets that supports *LIPA*

as the causal gene (P_{SMR} < 0.001 and P_{HEIDI} > 0.05, **Supplemental Table III**). Altogether, we provided strong statistical evidence pointing *LIPA* as the candidate causal gene at this locus.

Functional genomic data support monocytes and macrophages as the causal cell types

Functional regulatory variants often exert tissue- and cell type-specific effects to regulate the expression of their target genes.[29] Settling the causal tissue/cell types would improve our ability to understand the causal regulatory mechanisms and pathogenesis in a disease-relevant context.[29] We applied three strategies leveraging large scale transcriptomic and epigenomic datasets to confirm the involved cell types for the regulatory role of the *LIPA* CAD variants.

First, we queried the GTEx, the largest eQTL datasets containing 48 tissue types from ~900 healthy subjects.[22] The strongest *LIPA* eQTL association lies in whole blood, followed by spleen, visceral adipose, while liver and arteries that are also relevant to CAD pathogenesis showed weak association (**Figure IB**). Since tissues showing top eQTL signals consist of large immune cell populations, we next queried the BLUEPRINT datasets to further dissect which immune cell population shows stronger association.[23] Indeed, the strongest eQTL association for *LIPA* lies in monocytes, with neutrophils and T cells showing weak or absence of eQTL signals (**Figure 1C**).

Second, eQTL studies in diseased tissue allow the discovery of associations not identifiable in healthy tissues, likely due to disease-relevant cell type composition and changes in regulatory landscape. Leveraging the STARNET datasets that have nine metabolic tissue and cell types collected from ~600 CAD patients and ~150 healthy controls, including blood, liver, visceral abdominal adipose, subcutaneous fat, skeletal muscle, atherosclerotic aortic wall (AOR), pre/early-atherosclerotic mammary arteries (MAM), human monocyte-derived macrophages (HMDM), and foamy macrophages (HMDM loaded with ac-LDL),[14] we applied the same IGA pipeline to STARNET and CARDIoGRAMplusC4D GWAS datasets in each given tissue/cell type at this risk locus (500kb flanking gene *LIPA*). We confirmed that: (1) the strongest *LIPA* eQTLs exist in AOR (**Figure 1D**), blood (**Figure 1E**), and HMDM (**Figure 1F**, Coloc H_4 > 0.8 & P_{HEIDI} > 0.05 **Supplemental Table II and Table III**); (2) eQTL associations are also identified in the liver, visceral abdominal adipose, subcutaneous fat, and skeletal muscle (**Figure IC-IF**), however, SMR analyses indicated the likelihood that different causal variants (in high LD) regulated CAD and *LIPA* expression independently in these tissues (P_{HEIDI} < 0.05 **Supplemental Table III**). (3) no *LIPA* eQTL association was observed in MAM, the healthy arteries mainly consist of endothelial cells and vascular smooth muscles unlikely to have immune cell accumulation. These results together support that monocytes/macrophages, and foamy macrophages are likely to be the causal cell type. Our results confirmed that the *LIPA* eQTL associations are observed in AOR and liver in the STARNET datasets, but not arteries and liver in the GTEx dataset, supporting disease-specific regulatory mechanisms and the need to explore the involvement of disease-relevant cell types.

Indeed, although well powered, tissue-level eQTL studies provide limited insights into cell type-specific regulatory mechanisms. Single-cell ATAC-seq of human atherosclerotic plaque allows the identification of cell type-specific regulatory elements in a variety of cell types in the lesions. A recent scATAC-seq of

human atherosclerotic plaque datasets (n=41 subjects and 28,316 cells) strongly supported a myeloid-specific regulatory element that hosts rs1320496 as well as the lead *LIPA* SNP (rs1412444) associated with CAD.[30] The regulatory element was not detected in vascular smooth muscle cell-derived macrophage like cells nor any other cell types in the plaque, further supporting a myeloid-specific regulatory mechanism. In addition, in the STARNET dataset, rs1320496 was identified as the lead eQTL SNP ($P = 1.11\times10^{-11}$) for *LIPA* in foamy macrophages (**Figure 1G**). Taken together, current large-scale functional genomic datasets at bulk and single-cell level support monocytes and macrophages as the causal cell type for the regulatory effects of *LIPA* variants.

eQTL and enzyme activity-QTL in monocytes and macrophages support the directionality of the *LIPA* CAD variants with risk alleles associated with higher LIPA mRNA, protein, and enzyme activity

Upon establishing the causal cell types, it is important to confirm the directionality of the regulatory effects of the *LIPA* variants, *i.e.,* how the risk alleles associated with higher CAD risk link to *LIPA* expression in the causal cell types. Two previous eQTL cohorts[6, 7] established that the risk alleles (T) of rs1412444 and rs2246833 (in high LD with rs1412444, $r^2 = 0.985$) associated with increased *LIPA* mRNA in human monocytes. A recent study by Evans et al further confirmed that LIPA mRNA as well as enzyme activity were higher in human monocytes from the risk allele carriers of rs1412444 than the non-risk allele carriers (n=114).[19] In light of the strong eQTL signals in HMDM and foamy macrophages in the STARNET datasets and the important role of macrophages in atherosclerosis, the root cause of CAD, we set out to determine how LIPA variants may be associated with LIPA expression and enzyme activity in human macrophages.

Leveraging our cohort of HMDM samples from fully genotyped healthy subjects (**Supplemental Table IV**), we confirmed that in human HMDM, *LIPA* mRNA significantly increased by 1.42-fold and 1.57-fold in individuals with heterozygous risk allele (C/T) and with homozygous risk alleles (T/T), respectively, compared to non-risk allele carriers for rs1412444 (C/C) (**Figure 1H**). LIPA enzyme activity also significantly elevated in individuals having C/T and T/T genotypes by 36.94% and 47.00%, respectively, compared to the C/C genotype, suggesting that the *LIPA* CAD risks alleles may cause increased LIPA at both mRNA and enzyme activity level (**Figure 1I**). As shown in **Figure 1J-1K**, LIPA protein was also higher in the risk allele carriers. Thus, large functional genomic datasets and experimental validation support that risk alleles associated with higher CAD risk link to higher mRNA, protein, and enzyme activity of LIPA in both human monocytes and macrophages.

Experimental validation establishes the functional regulatory element and the functional variants, and the directionality of their effects

Connecting the variants to the target gene fully established the causality of the locus. We next set out to experimentally validate the regulatory elements and the functional variants at the *LIPA* locus that regulate *LIPA* mRNA expression, and consequently protein expression and enzyme activity. We applied four strategies (**Figure 2A**): (1) fine mapping to overlap prioritized variants with known histone modification

hallmarks and transcription factor binding in published ChIP-seq data in monocyte and macrophages; (2) high-resolution Tri-HiC to identify the enhancer-promoter regulatory loop within the *LIPA* locus in a cell type-specific manner; (3) luciferase assay followed by site-directed mutagenesis to validate the enhancer activities and the functional variant(s) *in vitro*; (4) Allele-specific binding and motif analyses to explore the molecular mechanisms of the regulatory effects of the functional variants.

Leveraging published histone modification and transcription factor ChIP-seq data in monocytes and macrophages,[31] we created a genome browser view to visualize the *LIPA* locus, including the prioritized SNPs (the GWAS lead SNP and SNPs in high LD) and the regulatory landscape. Several prioritized SNPs reside in enhancer landmarks and transcription factor binding sites. For example, a region containing rs1412444, rs1412445, and rs1320496 overlaps with binding sites for PU.1 and C/EBPβ, both are transcription factors important in myeloid differentiation (**Figure 2B**).[32-34] Also, rs2246833 resides in a region showing enhancer feature and C/EBPβ binding (**Figure 2B**). We therefore prioritize the rs1412444 region and rs2246833 region (highlighted in **Figure 2B**) for functional validation.

Enhancer and promoter looping represents a key mechanism of how functional variants regulate the transcription of their target gene.[29] We generated high-resolution Tri-HiC data in human monocytes and T cells to identify potential enhancer-promoter interaction within the *LIPA* locus at hundreds base pair-resolution.[35] Tri-HiC used three restriction enzymes for digestion (instead of one as used in many HiC methods, thus named "Tri"-HiC), resulting in 1.9-fold to 5.2-fold shorter fragments, thus reducing gaps of undigested intervals and improving detection.[35] Tri-HiC data revealed a strong interaction between the rs1412444 region and the *LIPA* promoter specifically in monocytes, but not T-cells (**Figure 2C**), consistent with eQTL data showing a lack of eQTL association in T-cell for the *LIPA* variants (**Figure 1C**).

To establish the causal variants within the enhancer region, we designed luciferase assay followed by site-directed mutagenesis to validate the enhancer activity and identify the alleles regulating the enhancer activity. DNA segments of the rs1412444 region and rs2246833 region were cloned into firefly luciferase expression vectors, and transfected to THP-1 monocytes or HEK cells. As shown in **Figure 2D**, the rs1412444 region showed strong enhancer activity in THP-1 monocytes, but no enhancer activity in HEK cells (**Figure IIA**), corroborating the Tri-HiC data supporting the interaction between the rs1412444 region and the *LIPA* promoter. An absence of enhancer activity of the rs1412444 region in HEK cells further supported a myeloid-specific regulatory mechanism of the enhancer element. The rs2246833 region did not show enhancer activity in either monocytes or HEK cells (**Figure 2D** and **Figure IIA**), consistent with the relatively weaker enhancer features as visualized in the genome browser landscape (**Figure 2B**).

We thus prioritized the rs1412444 region to identify the functional variants regulating the enhancer activity. Three SNPs, rs1412445, rs1320496 and rs1412444, in the rs1412444 region were prioritized for luciferase assay with site-directed mutagenesis because: (1) rs1412444 is the lead SNP in CAD GWAS (**Figure 1A**) and *LIPA* eQTL in AOR (**Figure 1D**); (2) rs1412445 is in perfect LD with rs1412444 (r^2=1); (3) rs1320496 shows the strongest signal for LIPA eQTL in HMDM and foamy macrophages (**Figure 1F and 1G**), though only in modest LD with SNP rs1412444 (r^2 = 0.6). Three major haplotypes are observed based on the genotypes of these three SNPs in our human cohort (**Supplemental Table V**), including

CCC (rs1412445-C, rs1320496-C, and rs1412444-C), CTC (rs1412445-C, rs1320496-T, and rs1412444-C), and TTT (rs1412445-T, rs1320496-T, and rs141244-T). A rare haplotype TTC (n=1) from the African American cohort was excluded. The luciferase vectors were constructed for the three haplotypes and luciferase assays were performed in THP-1 monocytes. As shown in **Figure 2E**, the CTC and CTT haplotypes led to increased enhancer activity compared with the CCC haplotype. Because rs1412444 and rs1412445 are in perfect LD ($r^2 = 1$), the individual contribution of rs1412445 and rs1320496 on *LIPA* expression and on CAD association were disentangled by employing interaction models and conditional analysis. Both SNPs demonstrate significant associations with *LIPA* expression (**Figure 2F**) and CAD (**Figure 2G**). Importantly, conditional analysis to identify independent signals suggests that the risk allele (T) of rs1320496 showed significant association with both *LIPA* expression and CAD when the entire effects of rs1412445 were removed from the data (eQTL $P = 3\times10^{-10}$, GWAS P = 0.03, **Figure 2F and 2G**). These results suggested that both rs1412445/rs1412444 and rs1320496 exert independent effects on *LIPA* expression and on CAD risk, supporting the additive effects of multiple variants within the same regulatory region.

Genetic variants may regulate the expression of their target genes by altering transcription factor binding. ChIP-seq data reveal a strong binding site to PU.1 within the rs1412444 region (**Figure 2B**). We hypothesized that the functional variants may regulate enhance activities of the genomic element via altering interaction with PU.1. The ENCODE PU.1 ChIP-seq reads in LCL cell line in two independent experiments were examined, with the rationale that an allele-specific binding (ASB) pattern in the ChIP-seq reads would suggest that a SNP at the locus influencing PU.1 binding. All three SNPs appeared to show allelic imbalance with risk alleles having higher binding activity to PU.1 than the non-risk alleles (**Figure 2H**). Among the three ASB SNPs, the risk allele (T) of rs1320496 directly changes the key nucleotide in the PU.1 binding DNA sequence (**Figure 2I**). Though we cannot dissect the regulatory effects individually for the three ASB SNPs due to their proximity (within a 150 bp region), rs1320496 was the only SNP predicted that the risk allele creates a PU.1 binding site.

In summary, our functional genomic studies established that the CAD GWAS variants at the *LIPA* locus confer increased risks of CAD via increasing the expression and enzyme activity of LIPA in monocytes and macrophages. We next sought to determine whether and how increased myeloid LIPA may influence the development of atherosclerosis.

Transgenic mouse studies demonstrate that myeloid-specific overexpression of *Lipa* promoted atherosclerosis

To establish the causality of the variant-to-function relationship for the *LIPA* locus and elucidate how increased myeloid *LIPA* impacts atherosclerosis *in vivo*, we generated myeloid-specific *Lipa* transgenic mice on C57BL/6 background ($LysMCre^{+/-}$,$Lipa^{fl/wt}$,$Ldlr^{-/-}$ hereafter referred as $Lipa^{Tg}$, **Figure IIIA**). Their corresponding littermates $LysMCre^{-/-}$,$Lipa^{fl/wt}$,$Ldlr^{-/-}$ (*Ctl*) were used as controls. The myeloid specificity and efficiency of *LysMCre*-mediated recombination is confirmed by quantifying the percentage of GFP^+ cells in different cell types and tissues because GFP serves as a reporter for *Lipa* overexpression. GFP^+ cells account for 36.2%, 22.0%, 34.8%, and 68.5% of $CD115^+$ cells in the blood, bone marrow (BM),

spleen, and peritoneum, respectively (**Figure IIIB**). In *Lipa*^{Tg} mice, 46.28% and 70.24% of Ly6G^{hi} neutrophils were GFP^{+} in the blood and BM, respectively (**Figure IIIC**). In CD3^{+} lymphocytes, the GFP^{+} cells were negligible (< 2.7%, **Figure IIID**) in *Lipa*^{Tg} mice, supporting myeloid-specific overexpression. The efficiency of *LysMCre* recombination is also consistent with previous reports on *LysMCre*-mediated transgenic overexpression mouse models.[36, 37]

The overexpression of *Lipa* was confirmed in bone marrow-derived macrophages (BMDM, **Figure IIIE-IIIJ**) and peritoneal macrophages (PM, **Figure IIIK-IIIP**) isolated from *Lipa*^{Tg} mice. In female mice, the mRNA and enzyme activity of LIPA increased by 1.41-fold (P = 0.033) and 21.03% (P = 0.034) in *Lipa*^{Tg} BMDM (**Figure IIIE-IIIF**) and 2.52-fold (P = 0.0001) and 24.04% (P = 0.012) in *Lipa*^{Tg} PM (**Figure IIIK-IIIL**) compared to *Ctl*, respectively. In male mice, the mRNA and enzyme activity of LIPA increased by 1.56-fold (P = 0.002) and 26.16% (P = 0.026) in *Lipa*^{Tg} BMDM (**Figure IIIG-IIIH**) and by 3.49-fold (P = 0.005) and 43.59 % (P = 0.0001) in *Lipa*^{Tg} PM (**Figure IIIM-IIIN**) compared to *Ctl*, respectively. Consistently, LIPA protein was significantly increased in both BMDM and PM (**Figure IIIO-IIIP**) in *Lipa*^{Tg} mice compared to *Ctl*. Despite the modest overexpression, the effect size of increased enzyme activity in *Lipa*^{Tg} BMDM and PM was comparable to the effect size of increased enzyme activity in HMDM of risk allele carriers (**Figure 1I**). The *Lipa*^{Tg} mice thus represent a valid model to investigate the causal effects of gain-of-function of LIPA as implicated in human functional genomic data.

To assess the effects of increased myeloid LIPA on atherosclerosis, the *Ctl* and *Lipa*^{Tg} mice were fed with a Western Diet (WD) for 16 weeks. We first assessed body weight, organ weight, and plasma lipid profile. Body weight gain did not differ between *Ctl* and *Lipa*^{Tg} mice (**Figure IVA** and **IVH** for males and females, respectively). Spleen and liver weights were also comparable (**Figure IVB-IVC** and **IVI-IVJ** for males and females, respectively). Plasma cholesterol levels were similar between *Ctl* and *Lipa*^{Tg} mice after 4h fasting (**Figure IVD** and **IVK** for males and females, respectively). Fast protein liquid chromatography (FPLC) assay also depicted comparable cholesterol levels in low-density lipoprotein (LDL) and high-density lipoprotein (HDL) fractions between *Ctl* and *Lipa*^{Tg} mice (**Figure IVE** and **IVL** for males and females, respectively). Female *Lipa*^{Tg} mice showed higher plasma triglyceride (**Figure IVF**) in both LDL and HDL fractions (**Figure IVG**), while the effects were not observed in male mice (**Figure IVM-IVN**). Overall, the myeloid LIPA overexpression did not alter weight gain or plasma cholesterol, consistent with the lack of association between *LIPA* variants and metabolic traits in human, although the effects of myeloid *Lipa*^{Tg} on triglyceride metabolism specifically in female mice on a WD require further examination.[38, 39]

Consistent with our human functional genomic discoveries, the atherosclerotic lesion size was significantly, though modestly, increased by 21.85% in *Lipa*^{Tg} female mice and 17.78% in *Lipa*^{Tg} male mice compared to the *Ctl* (**Figure 3A-3B**) fed with 16-week WD, supporting the pro-atherogenic role of *Lipa*^{Tg}. Importantly, the lesion size is positively correlated with LIPA activity in PM (**Figure. 3C**, P = 0.0143, r =0.04499), supporting the association between increased macrophage LIPA activity and atherogenesis. The percentage of necrotic core area (**Figure 3D**) and fibrous cap thickness (**Figure 3E**), markers of plaque stability,[40] did not show differences between genotypes. In accordance with the increased lesion size, *Lipa*^{Tg} significantly increased CD68^{+} macrophage area in the lesion in both sexes (**Figure 3F**). Elevated macrophage content in the plaque could be attributed to reduced turnover and/or increased

proliferation,[41, 42] while macrophage apoptosis and proliferation, determined by TUNEL (terminal deoxynucleotidyl transferase dUTP nick-end labelling) and Ki67, respectively, in CD68$^+$ region did not differ between two genotypes (**Figure 3G-3H**). We further confirmed that *Lipa^{Tg}* did not alter myelopoiesis in the blood and BM upon WD feeding (**Figure VA-VD**). Moreover, *Lipa^{Tg}* did not affect the percentage of hematopoietic progenitor cells in the BM (**Figure VE-VF**), supporting that the increased plaque macrophages were not due to increased myelopoiesis or hematopoiesis. Taken together, myeloid *Lipa* overexpression promotes atherosclerosis with an increased macrophage content in the lesion.

Single-cell RNA-seq data suggest a less foamy yet more pro-inflammatory transcriptomic profile in *Lipa^{Tg}* plaque macrophages

To gain further insights into the effects of *Lipa^{Tg}* on the phenotypic/functional heterogeneity of plaque macrophages, we carried out single-cell RNA-sequencing (scRNA-seq) analysis. Because the *LysMCre*-mediated recombination is not 100% for transgenic overexpression, we leverage this feature and separated CD45$^+$, GFP$^-$ (no *Lipa* overexpression) and CD45$^+$, GFP$^+$ (*Lipa* overexpression) cells from enzymatically dissociated aortas of *Lipa^{Tg}* mice fed with a WD for 16 weeks (**Figure 4A**). This design allows us to determine the difference between plaque macrophages with or without *Lipa* overexpression, yet were exposed to the same plaque microenvironment. Gating strategies for flow cytometry-based cell sorting were summarized in **Figure VIA**. Data analysis was performed using Seurat. Annotation of immune cell populations were done based on published scRNA-seq markers in meta-analysis atherosclerotic plaque cells.[43 44]

A total of twelve distinct cell types were identified, including macrophages (cluster 0, 1, 2, 4, and 5) marked by *Adgre1, Csf1r, Fcgr1*, and *Cd68*, monocyte/dendritic cells (cluster 6, 8, 10, and 11), B cells (cluster 7) marked by *Cd79, plac8*, and *Ebf1* (**Figure 4B**). There are also a small number of vascular smooth muscle cells (cluster 3) marked by *Acta2* and *Tagln*, and fibroblast cells (cluster 9) marked by *Dcn, Pi16, Mmp3,* and collagen markers) likely due to sorting-related contamination (**Figure 4B**). Importantly, the GFP$^+$ population has more than 95% of the cells annotated as macrophages or monocytes/dendritic cells, further confirming the myeloid-specific overexpression of *Lipa* in our model. We also validated that mRNA of *Lipa* was significantly higher in GFP$^+$ macrophages than GFP$^-$ macrophages sorted from aortas of *Lipa^{Tg}* mice (**Figure 4C**).

To evaluate the heterogeneity of plaque macrophages, we focused on the macrophage subpopulations based on their marker genes (**Figure 4D** and **Table VI**). Five subpopulations of plaque macrophage were identified in both GFP$^-$ and GFP$^+$ cells, including *Trem2*^{hi} macrophages (cluster 0), *Trem2*^{hi} foamy macrophages (cluster 1), resident-like macrophages (cluster 2, defined by higher expression of *Lyve1, F13a1, Cd163*, and *Pf4*),[45, 46] inflammatory macrophages (cluster 4, defined by higher expression of *Il1b, Ccr2,* and *Cxcl12*),[46, 47] and proliferating macrophages (cluster 5, defined by higher expression of *Mki67* and *Birc5*).[41, 48] Both Cluster 0 and Cluster 1 macrophages had relatively abundant expression of *Trem2, Cd9,* and *Spp1*. Compared to Trem2^{hi} non-foamy macrophages (cluster 0), *Trem2^{hi}* foamy macrophages (cluster 1) are enriched for *Fabp5*, *Gpnmb*, *Ctsb*, *Apoc1*, and *Atp6v0d2,* a signature resembling increased lipid metabolism and lysosomal biogenesis, thus inferred as foamy-like subpopulation.[43, 49] Notably, the

percentage of *Trem2*^{hi} foamy macrophages (cluster 1) is 36.00% in GFP^{-} macrophages while 17.32% in GFP^{+} macrophages, suggesting a lower proportion of foamy macrophages in GFP^{+} *Lipa* overexpressing plaque macrophages (**Figure 4E**, **Table VII**). The percentage of resident-like macrophages (cluster 2) and inflammatory macrophages (cluster 4) are 14.39% and 8.72% in GFP^{-} macrophages, while 33.89% and 13.55% in GFP^{+} macrophages, suggesting a higher proportion of resident-like and inflammatory macrophages in GFP^{+} *Lipa* overexpression plaque macrophages (**Figure 4E**, **Table VII**). Overall, the scRNA-seq data revealed heterogeneity within plaque macrophages with *Lipa*^{Tg} shifts macrophages toward a less foamy yet more pro-inflammatory transcriptome signature.

We merged subpopulations for GFP^{-} macrophages and GFP^{+} macrophages in Seurat to perform differential expression analysis followed by Ingenuity Pathway Analysis (IPA) to characterize the overall difference without or with *Lipa* overexpression. As shown in **Figure 4F**, multiple inflammation-related pathways, such as iNOS signaling, MIF regulation of innate immunity, role of hypercytokinemia/hyperchemokinemia in the pathogenesis of inflammation, TNFR1 signaling, interferon signaling, and chemokine signaling, were predicted to be activated in GFP^{+} macrophages. When performing differential expression analysis for each subpopulation, the *Trem2*^{hi} macrophages (cluster 0) demonstrated the most significant activation of inflammation-related pathways and upregulated expression of *Cxcl2* and *Ccl4* in GFP^{+} macrophages (**Figure VIB**). Thus, *Lipa*^{Tg} not only increased macrophage content in the plaque, but also altered the transcriptomic profile and heterogeneity of plaque macrophages.

Lipa^{Tg} led to less neutral lipid accumulation in macrophages while increased monocyte infiltration into the plaque

The scRNA-seq data suggest a less foamy transcriptomic signature in GFP^{+} *Lipa* overexpressing plaque macrophages. To validate at the functional level, we applied a flow cytometry-based method to characterize foamy macrophages (SSC^{hi}LipidTOX^{hi}) in plaque macrophages (CD45^{+}CD11b^{+}CD64^{+}) (**Figure 5A** and **Figure VIIA**).[50] In atherosclerotic plaques, the percentage of SSC^{hi}LipidTOX^{hi} foamy macrophages were similar between *Lipa*^{Tg} and *Ctl* mice (**Figure 5B**). Yet, the mean fluorescent intensity (MFI) of LipidTOX in foamy macrophages isolated from *Lipa*^{Tg} mice was significantly lower than foamy macrophages isolated from *Ctl* mice (**Figure 5C**), indicating reduced neutral lipid accumulation in *Lipa*^{Tg} foamy macrophages. We further confirmed that, in *Lipa*^{Tg} mice, GFP^{+} foamy macrophages had lower MFI of LipidTOX than GFP^{-} foamy macrophages (**Figure 5D**).

We also characterize the SSC^{hi}LipidTOX^{hi} foamy macrophages in PM (F4/80^{+}) isolated from *Ctl* and *Lipa*^{Tg} mice that fed with a WD for 16 weeks (**Figure 5E** and **Figure VIIB**). The percentage of foamy PM was significantly lower in *Lipa*^{Tg} mice compared to *Ctl* mice (**Figure 5F**). In foamy PM, the MFI of LipidTOX was also significantly lower in *Lipa*^{Tg} mice compared to *Ctl* mice (**Figure 5G**). Consistently, in *Lipa*^{Tg} mice, GFP^{+} foamy PM had lower MFI of LipidTOX than GFP^{-} foamy PM (**Figure 5H**). We therefore validated that *Lipa* overexpression indeed led to less neutral lipid accumulation.

The predicted activation of chemokine signaling in *Lipa* overexpressing plaque macrophages prompted us to hypothesize that the increased macrophage content in the lesion may be attributable to increased chemotaxis of circulating monocytes. To test the hypothesis, Ly6C^{hi} circulating monocytes were selectively labeled with fluorescent beads as illustrated in **Figure 5I** and as previously described.[51] Three days after labeling, the number of fluorescent beads in the macrophage area within the lesion, an implication of increased circulating monocyte infiltration into the plaque, was quantified. An increased number of beads was found in CD68^{+} macrophage area in *Lipa*^{Tg} mice compared to *Ctl* (**Figure 5J-5L**). The results support that increased chemokine signaling in the plaque may further exacerbates circulating monocyte infiltration, thus increasing plaque macrophage accumulation and representing a feedforward regulatory mechanism.

DISCUSSION

Despite more than a decade having passed since the first CAD GWAS was reported, successful translation of genetic associations into causal genes and pathways has been confined to a small subset of GWAS loci.[29] Many of the GWAS CAD variants are in or near genes known to cause Mendelian dyslipidemia (e.g., LDLR, APOB) or established molecular targets for lipid lowering and CAD therapies (e.g., HMGCR and PCSK9).[52] A number of genetic risk loci for CAD act through established CAD risk factors, such as lipid traits, which themselves have a significant genetic determination. Yet, many confirmed loci appear to act through novel mechanisms that are independent of traditional risk factors.[29] Elucidating these mechanisms is critical for a more complete understanding of CAD pathogenesis and identification of actionable therapeutic targets. *LIPA* is one of the CAD loci that is specifically associated with CAD,[2-12] but not with any of the lipid traits.[13] It is therefore of great interest to tackle the variant-to-function relationship for the *LIPA* locus and determine how altered *LIPA* expression causally impacts atherosclerosis through mechanisms beyond effects on plasma lipids. Here, using functional genomic approaches and experimental mouse models, we present evidence that *LIPA* is causal in CAD. Our results support that (1) *LIPA* mRNA, protein, and enzyme activity were higher in HMDM of CAD risk allele carriers; (2) the CAD GWAS lead SNP rs1412444 resides in an enhancer region that shows strong interaction with the *LIPA* promoter and hosts the functional SNPs regulating *LIPA* expression; (3) risk alleles of rs1412445/rs1412444 and rs1320496 led to increased *LIPA* expression and enhancer activity in a myeloid-specific manner; (4) risk allele of rs1320496 increased *LIPA* enhancer activity via creating a motif binding site for PU.1 and enhancing PU.1 binding; (5) myeloid-specific overexpression of *Lipa* aggravated atherosclerosis in *Ldlr*$^{-/-}$ mice without altering hypercholesterolemia; (6) *Lipa*-overexpressing macrophages were less foamy but more inflammatory. Taken together, these data demonstrate that increased *LIPA* in myeloid cells drives atherogenesis, a directionality consistent with human GWAS and eQTLs finding for the *LIPA* locus.[6-8]

Delineating the causal variants for a GWAS risk locus is often challenging, partly because most GWAS variants are noncoding and in high LD with multiple variants within the same locus. A coding variant rs1051338, which is in high LD with the LIPA GWAS variants, causes a nonsynonymous threonine to proline change within the signal peptide of LIPA protein. Because of the essential role of LIPA in

lysosomal lipid metabolism, the initial preliminary work and speculation were that rs1051338 was the causal variant leading to lower LIPA activity.[53] Further work by Evans et al confirmed that the nonsynonymous change within the signal peptide of LIPA protein did not affect protein trafficking, enzyme activity, or secretion.[19] In a larger cohort of human subjects, Evans et al also showed that the risk allele (C) of rs1051338 (in high LD with rs1412444, $r^2 = 0.86$) is associated with increased LIPA mRNA and enzyme activity in human monocytes.[19] Our work further supported the same directionality in human macrophages. We also demonstrated the myeloid-specific nature of the regulatory role of the *LIPA* CAD variants, i.e. the enhancer activity of the rs1412444 region is myeloid-specific, and the chromatin interaction between the *LIPA* enhancer and promoter is observed in monocytes, but not T-cell. Our work also established the functional role of rs1412444/rs1412445 and rs1320496. We, however, might have not identified all the functional SNPs at the *LIPA* locus without performing an unbiased screening covering all the variants within the locus.

Our findings that myeloid-specific *Lipa* overexpression exacerbates atherosclerosis is consistent with and supports the human functional genomic discoveries. As the only known acidic lipase in the lysosome, *LIPA* plays a critical role in intracellular lipid metabolism. Loss-of-function of *LIPA* is the cause of Mendelian disorders characterized by lysosomal neutral lipid accumulation in multiple tissues.[17, 54] Enzyme replacement therapy with recombinant LIPA protein has demonstrated efficacy and safety in patients with LIPA deficiency.[55] These findings have demonstrated the essential role of *LIPA* in lipid homeostasis and the benefits of supplementing LIPA when there is severe LIPA deficiency. However, the effects of further increasing *LIPA* above the normal physiological level and for a prolonged period of time remain elusive. Loss of function of LIPA led to hepatomegaly, prompting a hypothesis that overexpressing *LIPA* in the liver would prevent hepatic lipid accumulation. Yet, a recent study demonstrated that hepatic *LIPA* overexpression by AAV8 did not attenuate steatosis but unexpectedly exacerbated inflammation and immune cell infiltration in the liver of mice fed with a WD.[56] Our work using myeloid-specific *Lipa* overexpression mice also supports an increased atherosclerosis lesion and macrophage content. The results causally validate the human functional genomic evidence for this locus and informs the field that increasing myeloid LIPA may not be a therapeutically applicable for CAD, despite the essential role of LIPA in regulating lysosomal lipid metabolism.

Our scRNA-seq analyses suggest that $Lipa^{Tg}$ led to less foamy yet more inflammatory macrophages in the atherosclerotic lesion, which was confirmed by reduced neutral lipid accumulation in both plaque macrophages and PM in $Lipa^{Tg}$ mice. Increased monocyte infiltration into the lesion aligns with pathway analysis supporting the activation of chemokine signaling in $Lipa^{Tg}$ plaque macrophages. Lipid accumulation and exacerbated inflammation are central events in atherogenesis. Recent lipidomics and RNA-seq analyses support that foamy macrophages exhibit a “less-inflammatory” phenotype than their non-foamy counterparts.[50, 57] The molecular mechanisms of how $Lipa^{Tg}$ regulates cholesterol hemostasis and conveys a pro-inflammatory activity in the atherosclerotic lesion, and more broadly, the crosstalk between lipid metabolism and inflammatory response at the immuometabolism level warrants further studies.

In conclusion, our results established that *LIPA* risk alleles drive increased myeloid LIPA and aggravate atherosclerosis. The workflow and functional genomic resources applied in this study will also shed light on and accelerate the systematic interrogation of genetic contribution to CAD risks by monocytes and macrophages.

SOURCES OF FUNDING

The authors' research work has received funding from R00HL130574 and R01HL151611, and the Irving Scholar award through UL1TR001873 by the National Center for Advancing Translational Sciences (NCATS) and the National Institutes of Health (NIH) (to HZ), the American Heart Association Postdoctoral Fellowships 20POST35130003 (to FL), the Russell Berrie Diabetes Foundation Diabetes Scholar Program (to XW), and the American Heart Association Postdoctoral Fellowships 21POST829654 (to XW). The content in this manuscript is solely the responsibility of the authors and does not necessarily represent the official views of the NIH.

ACKNOWLEDGMENTS

We would like to acknowledge the NIH funding sources to the Columbia Center for Translational Immunology (CCTi) Flow Cytometry Core by grant number S10OD020056 and S10RR027050 and P30DK063608; the NIH-supported microscopy resources in the Center for Biologic Imaging, specifically the confocal microscope supported by grant number 1S10OD019973-01; the NIH/NCI Cancer Center Support Grant P30CA013696 for the use of resources at the Columbia Genome Center; the Columbia Stem Cell Initiative (CSCI) Flow Cytometry Core under the leadership of Michael Kissner. FACS cell sorting was performed with great help from Dr. Caisheng Lu, the Technical Director of the CCTi Flow Cytometry Core. Schematic figures were created with BioRender.com.

DISCLOSURES

The authors declare no competing interests.

FIGURES AND FIGURE LEGENDS

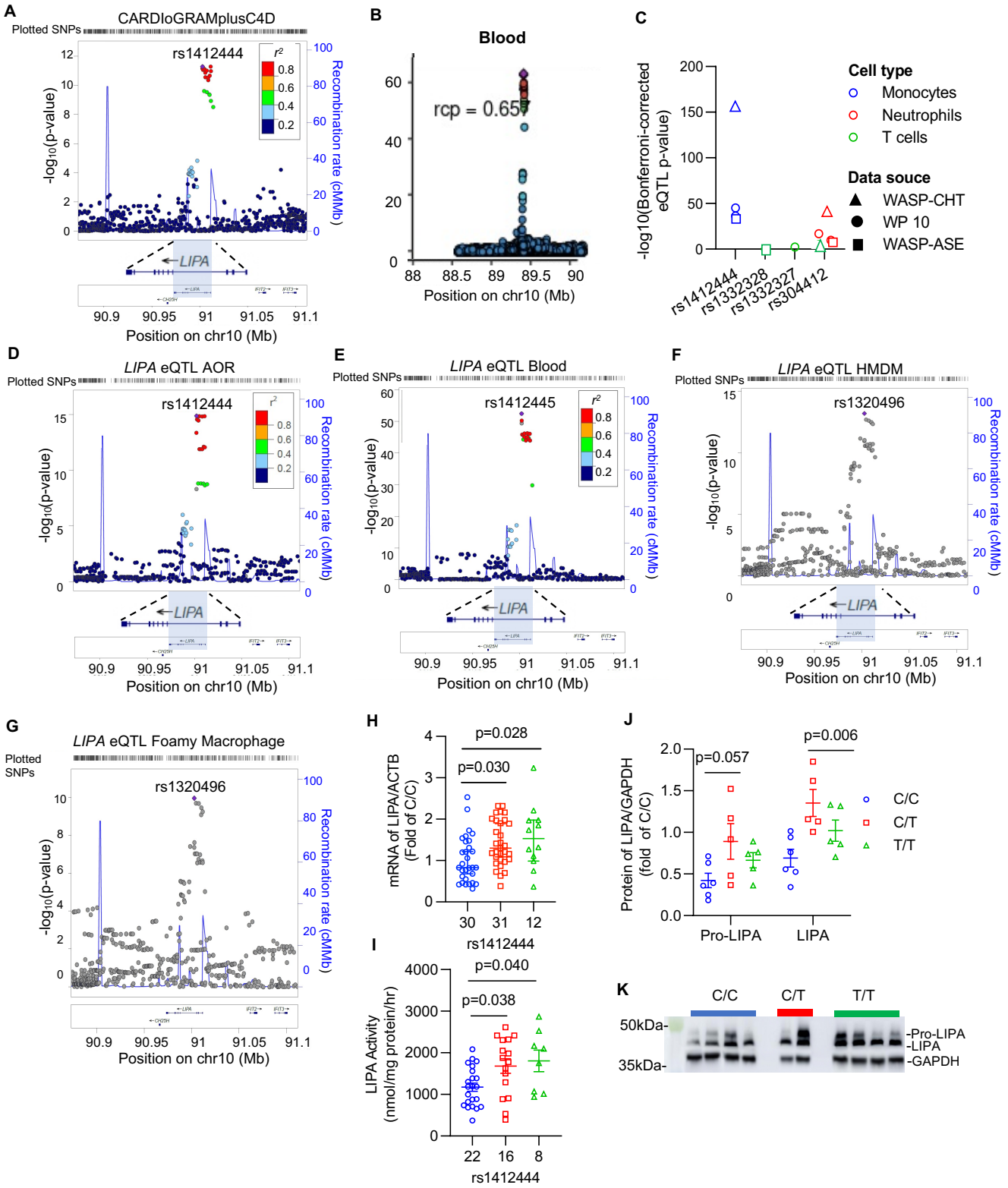

Figure 1. Risk alleles at the *LIPA* locus are associated with increased LIPA mRNA, activity, and protein in human monocytes-derived macrophages (HMDM).

A, LocusZoom plot of the *LIPA* locus (100 Mb flanking the *LIPA* gene) in the CARDIoGRAMplusC4D CAD GWAS. Single nucleotide polymorphisms (SNPs) in linkage disequilibrium (LD) with the GWAS lead SNP rs1412444 are color-coded based on r^2. **B,** Colocalization analysis by integrating CARDIoGRAMplusC4D GWAS dataset with the Genotype-Tissue Expression project (GTEx) statistics revealed that *LIPA* was the only nearby gene showed strong regional colocalization probability (crp = 0.657 in blood). **C,** Expression quantitative trait locus (eQTL) analysis of *LIPA* in the BLUEPRINT dataset supports the strongest signal in monocytes, not T cells or neutrophils. **D-G,** The LocusZoom plots visualizing *LIPA* eQTLs (100 kb flanking the *LIPA* gene) in atherosclerotic aortic wall (AOR, **D**), blood (**E**), HMDM (**F**), and foamy macrophages (acetylated-LDL loaded HMDM, **G**) In the Stockholm-Tartu Atherosclerosis Reverse Network Engineering Task (STARNET) dataset with nine cardiometabolic tissues/cell types from subjects with CAD. The most significant SNP is marked by purple diamond. Other SNPs in the region are color-coded by their LD with the top SNP according to pairwise r^2. **H-K**, The risk allele (T) of the CAD lead SNP rs1412444 is associated with increased *LIPA* mRNA (**H**), enzyme activity (**I**), and protein (**J, K**) in human HMDM (n = the number of subject). **K**, A representative Western Blot for quantification showing in (**J**). Data were analyzed by One-way ANOVA with Tukey's post-hoc and presented as mean ± SEM.

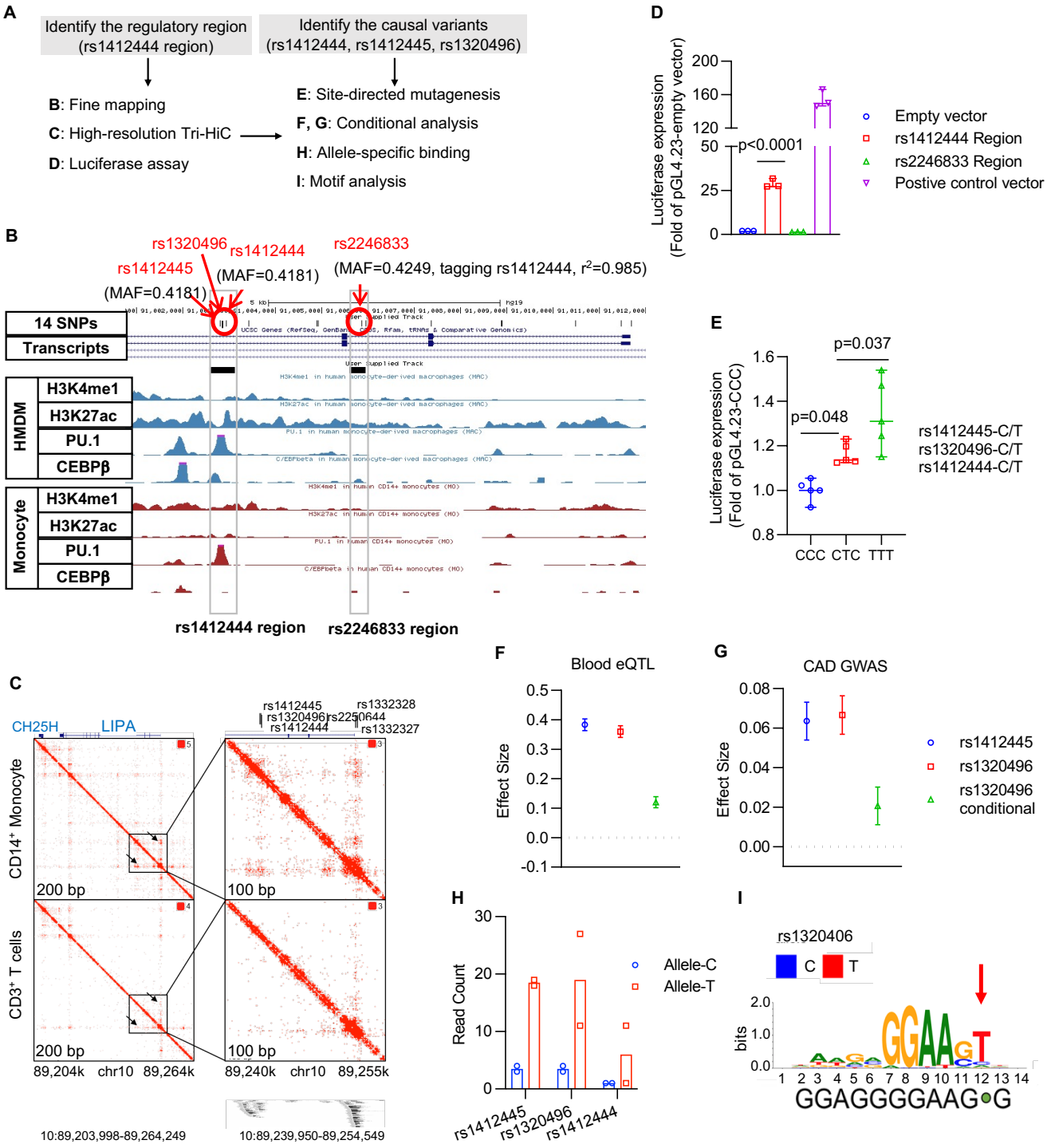

Figure 2. Rs1412444, rs1412445 and rs1320496 are identified as the functional variants that lead to higher *LIPA* expression in monocyte/macrophages via enhancing PU.1 binding.

A, Summary of study design. **B,** UCSC Genome Browser view of the *LIPA* locus showing the CAD GWAS lead SNP (rs1412444) and SNPs in high LD, and the regulatory landscape. The rs1412444 region and

rs2246833 region show the feature of enhancers (H3K4me1, H3K27ac) and binding of transcription factors (PU.1, C/EBPβ) in monocytes and HMDM. **C,** High-resolution Tri-HiC depicted interactions between the rs1412444 region and the *LIPA* promoter in human $CD14^+$ monocytes, but not in $CD3^+$ T cells. **D**, The rs1412444 region, but not the rs2246833 region, showed enhancer activity by luciferase assay in THP1 monocytes. (n = 3 independent experiments with 3 technical replicates, data are presented as median ± 95% CI). **E,** Site-directed mutagenesis and luciferase assay support that the risk haplotype (rs1412445-T, rs1320496-T, and rs1412444-T) led to increased enhancer activity. The rs1412444 and rs1412445 have perfect LD with $r^2 = 1$. The assay was therefore analyzed according to the haplotype. (n = 5 independent experiments with 3 technical replicates, data are presented as median ± 95% CI). **F-G,** The effects of individual SNPs within the rs1412444 region were disentangled by conditional analysis, showing that both rs1412445/rs1412444 and rs1320496 exert independent effects on *LIPA* expression and on CAD risk. **H,** The count of PU.1 (encoded by *SPI1*) reads aligned to the reference (C, blue) and the alternative (T, red) alleles in the ENCODE PU.1 ChIP-seq data of LCL cell line (n = 2 independent ChIP-seq experiments). All three SNPs appear to show an allele-specific binding (ASB) pattern with the risk alleles (T) having stronger binding effects to PU.1 compared to non-risk alleles. **I,** Motif analysis supports that the risk allele of rs1320496 creates a PU.1 binding site.

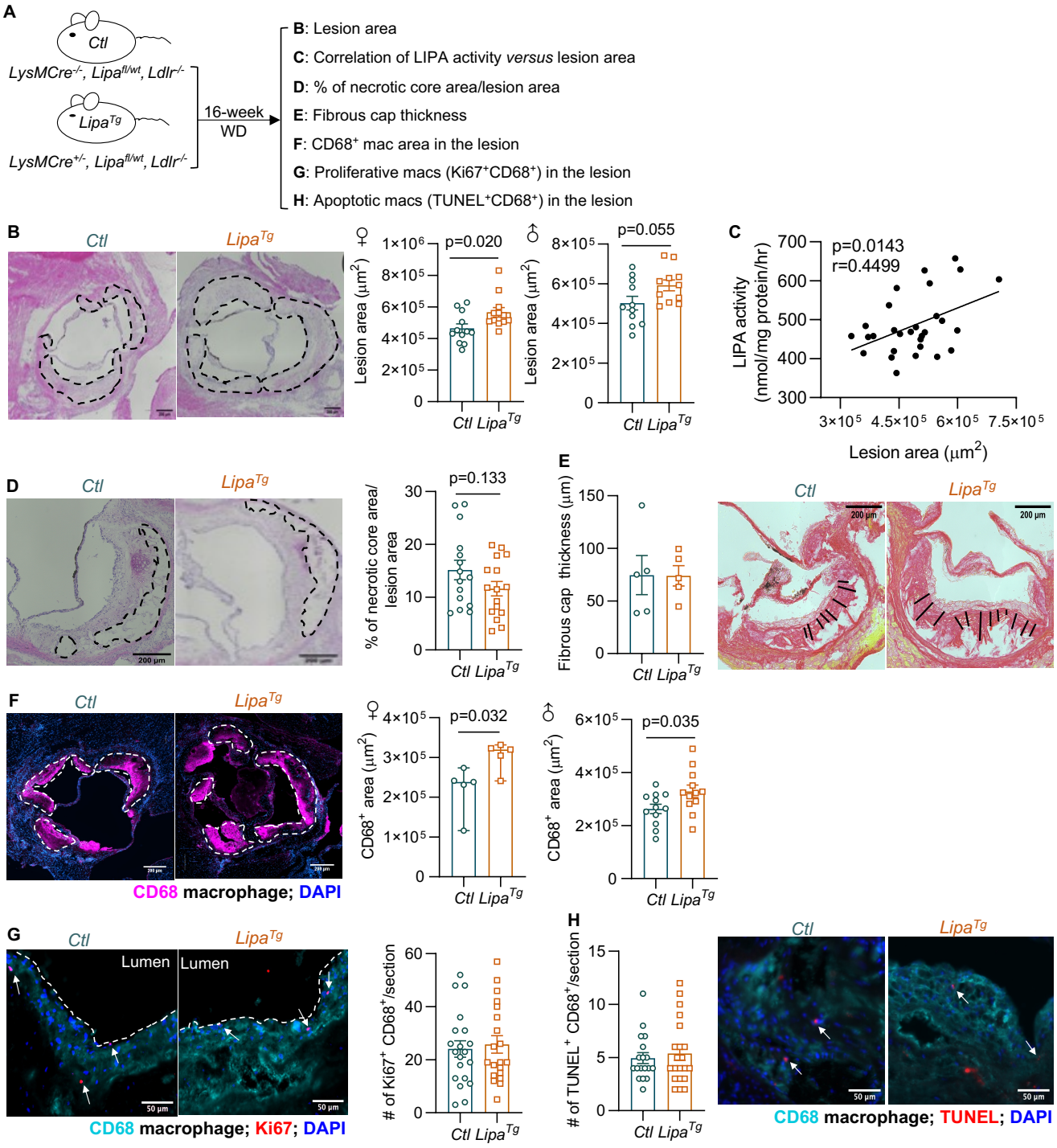

Figure 3. Myeloid-specific *Lipa* overexpression promotes atherosclerosis in *Ldlr*$^{-/-}$ mice.

A, Schematics of the study design: *Ctl* (*LysMCre*$^{-/-}$, *Lipa*$^{fl/wt}$, *Ldlr*$^{-/-}$) and *Lipa*^{Tg} (*LysMCre*$^{+/-}$, *Lipa*$^{fl/wt}$, *Ldlr*$^{-/-}$) mice were fed with a Western diet (WD) for 16 weeks. The atherosclerotic lesion size, plaque stability, and macrophage content in the aortic sinus were quantified. **B,** *Lipa*^{Tg} modestly but significantly increased

atherosclerotic lesion size in both female (left, *Ctl*, n= 12 mice; *Lipa*^{Tg}, n=14 mice, median ± 95% CI) and male mice (right, n = 11 mice). Scale bar = 200 μm. **C,** Atherosclerotic lesion size significantly and positively correlated with LIPA enzyme activity in PM (two-tailed Pearson's correlation analysis, P = 0.014, *r* = 0.4499). **D**, H&E staining revealed no differences in the percentage of necrotic core area (*Ctl*, n = 14 mice; *Lipa*^{Tg}, n = 15 mice, mixed sexes) between the two genotypes. **E**, Sirius red staining showed comparable fibrous cap thickness between the two groups (n = 5 male mice). **F**, immunofluorescent (IF) staining showed that *Lipa*^{Tg} significantly increased CD68^{+} macrophage area in the lesion compared to *Ctl* (left, n = 5 female mice, median ± 95% CI; right, n = 12 male mice). Scale bar, 200 μm. **G-H**, *Lipa*^{Tg} did not affect plaque macrophage proliferation (**G**, n = 20 mice, mixed sexes, median ± 95% CI) nor apoptosis (**H**, n = 21 mice, mixed sexes, median ± 95% CI) of CD68^{+} macrophages. Scale bars, 50 μm. Data are shown as mean ± SEM unless specifically stated.

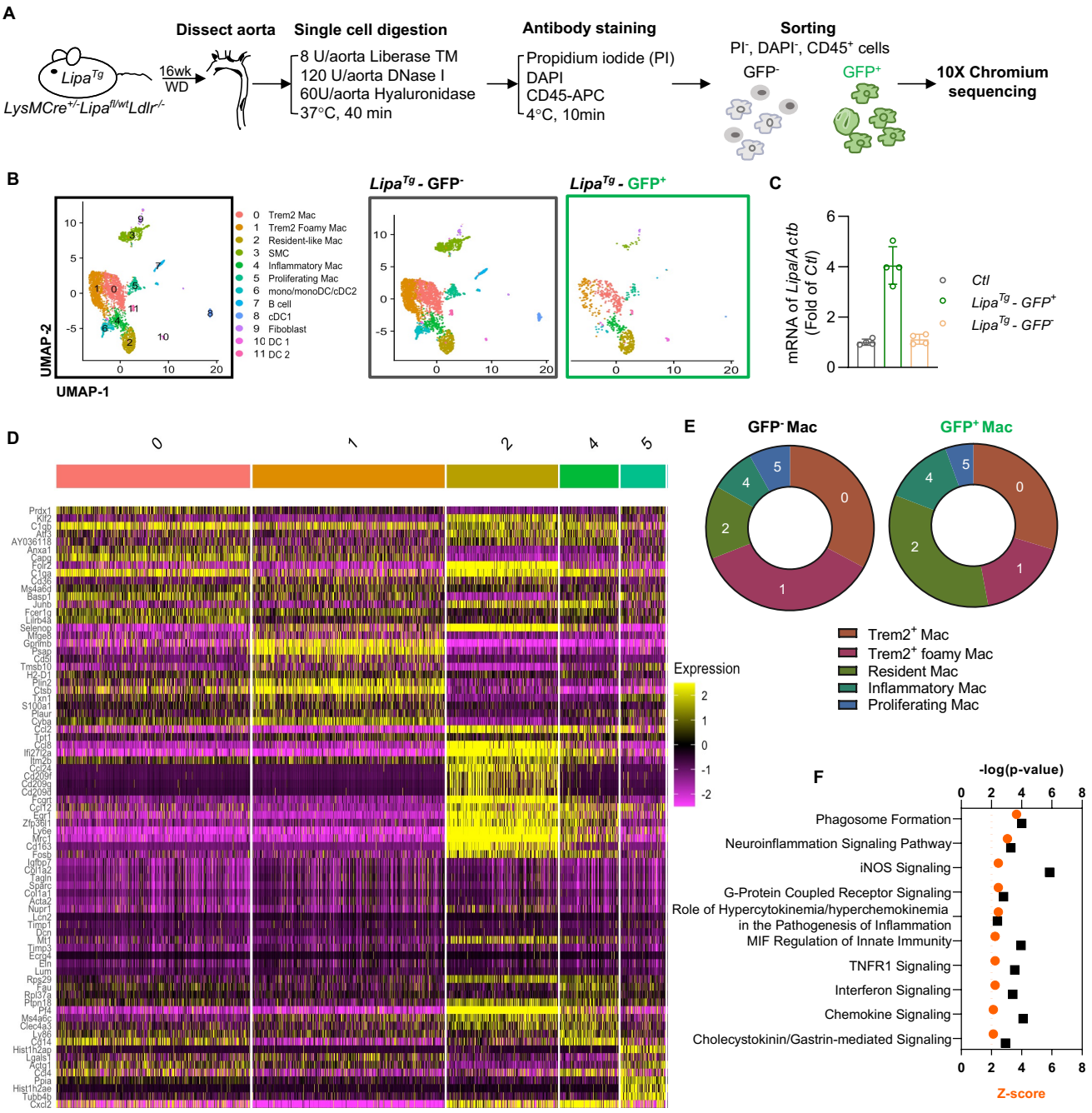

Figure 4. Single-cell RNA-seq data suggest a less foamy yet more pro-inflammatory transcriptomic profile in *Lipa*^{Tg} plaque macrophages.

A, Schematics of the scRNA-seq experiment profiling the CD45$^+$ GFP$^-$ and CD45$^+$ GFP$^+$ cells isolated from the atherosclerotic plaques of *Lipa*^{Tg} mice fed with 16-week of WD using 10X Chromium. **B**, Uniform Manifold Approximation and Projection (UMAP) plots of CD45$^+$ cells isolated from aortas of *Lipa*^{Tg} mice (n = 5 male mice pooled). A total of twelve cell clusters including five macrophage subpopulations (cluster 0, 1, 2, 4, and 5) were identified. **C,** qPCR confirmed that mRNA of *Lipa* is significantly higher in GFP$^+$

macrophages isolated from *Lipa*^{Tg} mice compared to GFP^{-} macrophages isolated from *Lipa*^{Tg} mice, and macrophages from the *Ctl* mice, confirming the sorting strategy and the overexpression efficiency ($P < 0.001$, n = 4 independent experiments with each experiment performed in pooled macrophages from 2-3 mice, and with 2 technical replicates per experiment). **D,** Heatmap of top 15 differentially expressed (DE) genes in each macrophage subpopulation to support the annotation of the subpopulation. **E**, Proportion of GFP^{-} (left) and GFP^{+} (right) cells in each macrophage subpopulations. GFP^{+} macrophages contributed to a greater portion of resident-like macrophages (cluster 2) and inflammatory macrophages (cluster 4) yet lesser portion of *Trem2*^{hi} foamy macrophages (cluster 1) in the plaque macrophages. **F,** Ingenuity Pathway Analysis (IPA) of GFP^{+} *versus* GFP^{-} macrophages. Inflammation-related pathways were predicted to be significantly activated with a positive z-score in GFP^{+} macrophages.

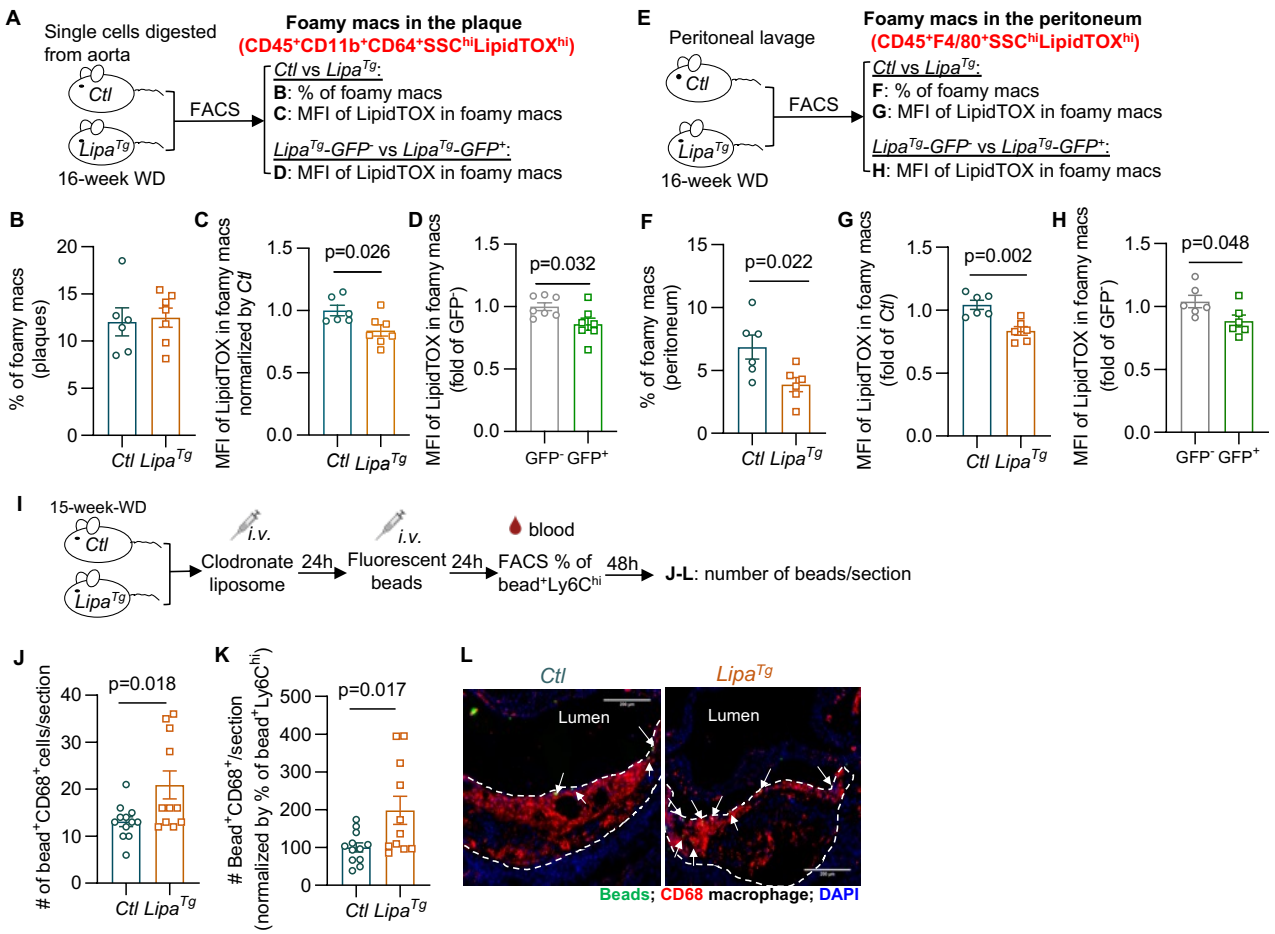

Figure 5. *Lipa^Tg* led to less neutral lipid accumulation in macrophages while increased monocyte infiltration into the plaque.

A, Schematics of a flow cytometry-based method to characterize foamy macrophages ($CD45^+CD11b^+CD64^+SSC^{hi}LipidTOX^{hi}$) in atherosclerotic plaques. **B,** Percentage of foamy macrophages in total macrophages in the aortas. **C**, Mean fluorescent intensity (MFI) of LipidTOX in foamy macrophages in the aortas of *Ctl* and *Lipa^Tg* mice. **D,** MFI of LipidTOX in GFP^+ and GFP^- foamy macrophages in the aortas of *Lipa^Tg* mice. **B-D**, n = 6 male mice for *Ctl*; n= 7 male mice for *Lipa^Tg*; mean ± SEM. **E,** Schematics of study design to characterize foamy peritoneal macrophages (PM) ($CD45^+F4/80^+SSC^{hi}LipidTOX^{hi}$). **F,** Percentage of foamy PM. **G,** MFI of LipidTOX in foamy PM in *Ctl* and *Lipa^Tg* mice. **H,** MFI of LipidTOX in GFP^+ and GFP^- foamy PM in *Lipa^Tg* mice. **F-H**, n = 6 male mice; mean ± SEM. **I,** Schematics of beads assay assessing monocyte infiltration into the plaque. Briefly, $Ly6C^{hi}$ monocytes in the blood were selectively labeled with fluorescent beads by transiently depleting circulating monocytes with clodronate liposome injection. The beads incorporation rate in $Ly6C^{hi}$ monocytes was quantified by flow cytometry 24 h after beads injection. Three days after beads injection, the number of beads in $CD68^+$ area of atherosclerotic lesion was quantified. **J,** The number of beads in $CD68^+$ area per section. **K,** The number of beads in $CD68^+$ area per section normalized by the percentage of $bead^+$ $Ly6C^{hi}$ monocytes in the blood. **L,** Representative immunofluorescent staining of $beads^+$ (green) macrophages

(red) in the lesion. Scale bars, 200 μm. **J-K,** n = 8 female, 4 male in *Ctl* mice; n = 8 female, 3 male in *Lipa*^{Tg} mice; two sections were quantified for each mouse, mean ± SEM.

REFERENCES

1. McPherson R and Tybjaerg-Hansen A. Genetics of Coronary Artery Disease. *Circulation Research*. 2016;118:564-578.
2. van der Harst P and Verweij N. Identification of 64 Novel Genetic Loci Provides an Expanded View on the Genetic Architecture of Coronary Artery Disease. *Circ Res*. 2018;122:433-443.
3. Nikpay M, Goel A, Won HH, Hall LM, Willenborg C, Kanoni S, Saleheen D, Kyriakou T, Nelson CP, Hopewell JC, Webb TR, Zeng L, Dehghan A, Alver M, Armasu SM, Auro K, Bjonnes A, Chasman DI, Chen S, Ford I, Franceschini N, Gieger C, Grace C, Gustafsson S, Huang J, Hwang SJ, Kim YK, Kleber ME, Lau KW, Lu X, Lu Y, Lyytikainen LP, Mihailov E, Morrison AC, Pervjakova N, Qu L, Rose LM, Salfati E, Saxena R, Scholz M, Smith AV, Tikkanen E, Uitterlinden A, Yang X, Zhang W, Zhao W, de Andrade M, de Vries PS, van Zuydam NR, Anand SS, Bertram L, Beutner F, Dedoussis G, Frossard P, Gauguier D, Goodall AH, Gottesman O, Haber M, Han BG, Huang J, Jalilzadeh S, Kessler T, Konig IR, Lannfelt L, Lieb W, Lind L, Lindgren CM, Lokki ML, Magnusson PK, Mallick NH, Mehra N, Meitinger T, Memon FU, Morris AP, Nieminen MS, Pedersen NL, Peters A, Rallidis LS, Rasheed A, Samuel M, Shah SH, Sinisalo J, Stirrups KE, Trompet S, Wang L, Zaman KS, Ardissino D, Boerwinkle E, Borecki IB, Bottinger EP, Buring JE, Chambers JC, Collins R, Cupples LA, Danesh J, Demuth I, Elosua R, Epstein SE, Esko T, Feitosa MF, Franco OH, Franzosi MG, Granger CB, Gu D, Gudnason V, Hall AS, Hamsten A, Harris TB, Hazen SL, Hengstenberg C, Hofman A, Ingelsson E, Iribarren C, Jukema JW, Karhunen PJ, Kim BJ, Kooner JS, Kullo IJ, Lehtimaki T, Loos RJF, Melander O, Metspalu A, Marz W, Palmer CN, Perola M, Quertermous T, Rader DJ, Ridker PM, Ripatti S, Roberts R, Salomaa V, Sanghera DK, Schwartz SM, Seedorf U, Stewart AF, Stott DJ, Thiery J, Zalloua PA, O'Donnell CJ, Reilly MP, Assimes TL, Thompson JR, Erdmann J, Clarke R, Watkins H, Kathiresan S, McPherson R, Deloukas P, Schunkert H, Samani NJ and Farrall M. A comprehensive 1,000 Genomes-based genome-wide association meta-analysis of coronary artery disease. *Nat Genet*. 2015;47:1121-1130.
4. Koyama S, Ito K, Terao C, Akiyama M, Horikoshi M, Momozawa Y, Matsunaga H, Ieki H, Ozaki K, Onouchi Y, Takahashi A, Nomura S, Morita H, Akazawa H, Kim C, Seo JS, Higasa K, Iwasaki M, Yamaji T, Sawada N, Tsugane S, Koyama T, Ikezaki H, Takashima N, Tanaka K, Arisawa K, Kuriki K, Naito M, Wakai K, Suna S, Sakata Y, Sato H, Hori M, Sakata Y, Matsuda K, Murakami Y, Aburatani H, Kubo M, Matsuda F, Kamatani Y and Komuro I. Population-specific and trans-ancestry genome-wide analyses identify distinct and shared genetic risk loci for coronary artery disease. *Nat Genet*. 2020;52:1169-1177.
5. Tcheandjieu C, Zhu X, Hilliard AT, Clarke SL, Napolioni V, Ma S, Lee KM, Fang H, Chen F, Lu Y, Tsao NL, Raghavan S, Koyama S, Gorman BR, Vujkovic M, Klarin D, Levin MG, Sinnott-Armstrong N, Wojcik GL, Plomondon ME, Maddox TM, Waldo SW, Bick AG, Pyarajan S, Huang J, Song R, Ho YL, Buyske S, Kooperberg C, Haessler J, Loos RJF, Do R, Verbanck M, Chaudhary K, North KE, Avery CL, Graff M, Haiman CA, Le Marchand L, Wilkens LR, Bis JC, Leonard H, Shen B, Lange LA, Giri A, Dikilitas O, Kullo IJ, Stanaway IB, Jarvik GP, Gordon AS, Hebbring S, Namjou B, Kaufman KM, Ito K, Ishigaki K, Kamatani Y, Verma SS, Ritchie MD, Kember RL, Baras A, Lotta LA, Regeneron Genetics C, Consortium CAD, Biobank J, Million Veteran P, Kathiresan S, Hauser ER, Miller DR, Lee JS, Saleheen D, Reaven PD, Cho K, Gaziano JM, Natarajan P, Huffman JE, Voight BF, Rader DJ, Chang KM, Lynch JA, Damrauer SM, Wilson PWF, Tang H, Sun YV, Tsao PS, O'Donnell CJ and Assimes TL. Large-scale genome-wide association study of coronary artery disease in genetically diverse populations. *Nat Med*. 2022;28:1679-1692.
6. Consortium IKC. Large-scale gene-centric analysis identifies novel variants for coronary artery disease. *PLoS Genet*. 2011;7:e1002260.
7. Wild PS, Zeller T, Schillert A, Szymczak S, Sinning CR, Deiseroth A, Schnabel RB, Lubos E, Keller T, Eleftheriadis MS, Bickel C, Rupprecht HJ, Wilde S, Rossmann H, Diemert P, Cupples LA, Perret C, Erdmann J, Stark K, Kleber ME, Epstein SE, Voight BF, Kuulasmaa K, Li M, Schafer AS, Klopp N, Braund PS, Sager HB, Demissie S, Proust C, Konig IR, Wichmann HE, Reinhard W, Hoffmann MM, Virtamo J, Burnett MS, Siscovick D, Wiklund PG, Qu L, El Mokthari NE, Thompson JR, Peters A, Smith AV, Yon E,

Baumert J, Hengstenberg C, Marz W, Amouyel P, Devaney J, Schwartz SM, Saarela O, Mehta NN, Rubin D, Silander K, Hall AS, Ferrieres J, Harris TB, Melander O, Kee F, Hakonarson H, Schrezenmeir J, Gudnason V, Elosua R, Arveiler D, Evans A, Rader DJ, Illig T, Schreiber S, Bis JC, Altshuler D, Kavousi M, Witteman JC, Uitterlinden AG, Hofman A, Folsom AR, Barbalic M, Boerwinkle E, Kathiresan S, Reilly MP, O'Donnell CJ, Samani NJ, Schunkert H, Cambien F, Lackner KJ, Tiret L, Salomaa V, Munzel T, Ziegler A and Blankenberg S. A genome-wide association study identifies LIPA as a susceptibility gene for coronary artery disease. *Circulation Cardiovascular genetics*. 2011;4:403-12.

8. Coronary Artery Disease Genetics C. A genome-wide association study in Europeans and South Asians identifies five new loci for coronary artery disease. *Nat Genet*. 2011;43:339-44.

9. Consortium CAD, Deloukas P, Kanoni S, Willenborg C, Farrall M, Assimes TL, Thompson JR, Ingelsson E, Saleheen D, Erdmann J, Goldstein BA, Stirrups K, Konig IR, Cazier JB, Johansson A, Hall AS, Lee JY, Willer CJ, Chambers JC, Esko T, Folkersen L, Goel A, Grundberg E, Havulinna AS, Ho WK, Hopewell JC, Eriksson N, Kleber ME, Kristiansson K, Lundmark P, Lyytikainen LP, Rafelt S, Shungin D, Strawbridge RJ, Thorleifsson G, Tikkanen E, Van Zuydam N, Voight BF, Waite LL, Zhang W, Ziegler A, Absher D, Altshuler D, Balmforth AJ, Barroso I, Braund PS, Burgdorf C, Claudi-Boehm S, Cox D, Dimitriou M, Do R, Consortium D, Consortium C, Doney AS, El Mokhtari N, Eriksson P, Fischer K, Fontanillas P, Franco-Cereceda A, Gigante B, Groop L, Gustafsson S, Hager J, Hallmans G, Han BG, Hunt SE, Kang HM, Illig T, Kessler T, Knowles JW, Kolovou G, Kuusisto J, Langenberg C, Langford C, Leander K, Lokki ML, Lundmark A, McCarthy MI, Meisinger C, Melander O, Mihailov E, Maouche S, Morris AD, Muller-Nurasyid M, Mu TC, Nikus K, Peden JF, Rayner NW, Rasheed A, Rosinger S, Rubin D, Rumpf MP, Schafer A, Sivananthan M, Song C, Stewart AF, Tan ST, Thorgeirsson G, van der Schoot CE, Wagner PJ, Wellcome Trust Case Control C, Wells GA, Wild PS, Yang TP, Amouyel P, Arveiler D, Basart H, Boehnke M, Boerwinkle E, Brambilla P, Cambien F, Cupples AL, de Faire U, Dehghan A, Diemert P, Epstein SE, Evans A, Ferrario MM, Ferrieres J, Gauguier D, Go AS, Goodall AH, Gudnason V, Hazen SL, Holm H, Iribarren C, Jang Y, Kahonen M, Kee F, Kim HS, Klopp N, Koenig W, Kratzer W, Kuulasmaa K, Laakso M, Laaksonen R, Lee JY, Lind L, Ouwehand WH, Parish S, Park JE, Pedersen NL, Peters A, Quertermous T, Rader DJ, Salomaa V, Schadt E, Shah SH, Sinisalo J, Stark K, Stefansson K, Tregouet DA, Virtamo J, Wallentin L, Wareham N, Zimmermann ME, Nieminen MS, Hengstenberg C, Sandhu MS, Pastinen T, Syvanen AC, Hovingh GK, Dedoussis G, Franks PW, Lehtimaki T, Metspalu A, Zalloua PA, Siegbahn A, Schreiber S, Ripatti S, Blankenberg SS, Perola M, Clarke R, Boehm BO, O'Donnell C, Reilly MP, Marz W, Collins R, Kathiresan S, Hamsten A, Kooner JS, Thorsteinsdottir U, Danesh J, Palmer CN, Roberts R, Watkins H, Schunkert H and Samani NJ. Large-scale association analysis identifies new risk loci for coronary artery disease. *Nat Genet*. 2013;45:25-33.

10. Lee JY, Lee BS, Shin DJ, Woo Park K, Shin YA, Joong Kim K, Heo L, Young Lee J, Kyoung Kim Y, Jin Kim Y, Bum Hong C, Lee SH, Yoon D, Jung Ku H, Oh IY, Kim BJ, Lee J, Park SJ, Kim J, Kawk HK, Lee JE, Park HK, Lee JE, Nam HY, Park HY, Shin C, Yokota M, Asano H, Nakatochi M, Matsubara T, Kitajima H, Yamamoto K, Kim HL, Han BG, Cho MC, Jang Y, Kim HS, Euy Park J and Lee JY. A genome-wide association study of a coronary artery disease risk variant. *J Hum Genet*. 2013;58:120-6.

11. Vargas-Alarcon G, Posadas-Romero C, Villarreal-Molina T, Alvarez-Leon E, Angeles J, Vallejo M, Posadas-Sanchez R, Cardoso G, Medina-Urrutia A and Kimura-Hayama E. Single nucleotide polymorphisms within LIPA (Lysosomal Acid Lipase A) gene are associated with susceptibility to premature coronary artery disease. a replication in the genetic of atherosclerotic disease (GEA) Mexican study. *PLoS One*. 2013;8:e74703.

12. Matsunaga H, Ito K, Akiyama M, Takahashi A, Koyama S, Nomura S, Ieki H, Ozaki K, Onouchi Y, Sakaue S, Suna S, Ogishima S, Yamamoto M, Hozawa A, Satoh M, Sasaki M, Yamaji T, Sawada N, Iwasaki M, Tsugane S, Tanaka K, Arisawa K, Ikezaki H, Takashima N, Naito M, Wakai K, Tanaka H, Sakata Y, Morita H, Sakata Y, Matsuda K, Murakami Y, Akazawa H, Kubo M, Kamatani Y and Komuro I. Transethnic Meta-Analysis of Genome-Wide Association Studies Identifies Three New Loci and Characterizes Population-Specific Differences for Coronary Artery Disease. *Circ Genom Precis Med*. 2020;13:e002670.

13. Willer CJ, Schmidt EM, Sengupta S, Peloso GM, Gustafsson S, Kanoni S, Ganna A, Chen J, Buchkovich ML, Mora S, Beckmann JS, Bragg-Gresham JL, Chang HY, Demirkan A, Den Hertog HM, Do R, Donnelly LA, Ehret GB, Esko T, Feitosa MF, Ferreira T, Fischer K, Fontanillas P, Fraser RM, Freitag DF, Gurdasani D, Heikkila K, Hypponen E, Isaacs A, Jackson AU, Johansson A, Johnson T, Kaakinen M, Kettunen J, Kleber ME, Li X, Luan J, Lyytikainen LP, Magnusson PK, Mangino M, Mihailov E, Montasser ME, Muller-Nurasyid M, Nolte IM, O'Connell JR, Palmer CD, Perola M, Petersen AK, Sanna S, Saxena R, Service SK, Shah S, Shungin D, Sidore C, Song C, Strawbridge RJ, Surakka I, Tanaka T, Teslovich TM, Thorleifsson G, Van den Herik EG, Voight BF, Volcik KA, Waite LL, Wong A, Wu Y, Zhang W, Absher D, Asiki G, Barroso I, Been LF, Bolton JL, Bonnycastle LL, Brambilla P, Burnett MS, Cesana G, Dimitriou M, Doney AS, Doring A, Elliott P, Epstein SE, Eyjolfsson GI, Gigante B, Goodarzi MO, Grallert H, Gravito ML, Groves CJ, Hallmans G, Hartikainen AL, Hayward C, Hernandez D, Hicks AA, Holm H, Hung YJ, Illig T, Jones MR, Kaleebu P, Kastelein JJ, Khaw KT, Kim E, Klopp N, Komulainen P, Kumari M, Langenberg C, Lehtimaki T, Lin SY, Lindstrom J, Loos RJ, Mach F, McArdle WL, Meisinger C, Mitchell BD, Muller G, Nagaraja R, Narisu N, Nieminen TV, Nsubuga RN, Olafsson I, Ong KK, Palotie A, Papamarkou T, Pomilla C, Pouta A, Rader DJ, Reilly MP, Ridker PM, Rivadeneira F, Rudan I, Ruokonen A, Samani N, Scharnagl H, Seeley J, Silander K, Stancakova A, Stirrups K, Swift AJ, Tiret L, Uitterlinden AG, van Pelt LJ, Vedantam S, Wainwright N, Wijmenga C, Wild SH, Willemsen G, Wilsgaard T, Wilson JF, Young EH, Zhao JH, Adair LS, Arveiler D, Assimes TL, Bandinelli S, Bennett F, Bochud M, Boehm BO, Boomsma DI, Borecki IB, Bornstein SR, Bovet P, Burnier M, Campbell H, Chakravarti A, Chambers JC, Chen YD, Collins FS, Cooper RS, Danesh J, Dedoussis G, de Faire U, Feranil AB, Ferrieres J, Ferrucci L, Freimer NB, Gieger C, Groop LC, Gudnason V, Gyllensten U, Hamsten A, Harris TB, Hingorani A, Hirschhorn JN, Hofman A, Hovingh GK, Hsiung CA, Humphries SE, Hunt SC, Hveem K, Iribarren C, Jarvelin MR, Jula A, Kahonen M, Kaprio J, Kesaniemi A, Kivimaki M, Kooner JS, Koudstaal PJ, Krauss RM, Kuh D, Kuusisto J, Kyvik KO, Laakso M, Lakka TA, Lind L, Lindgren CM, Martin NG, Marz W, McCarthy MI, McKenzie CA, Meneton P, Metspalu A, Moilanen L, Morris AD, Munroe PB, Njolstad I, Pedersen NL, Power C, Pramstaller PP, Price JF, Psaty BM, Quertermous T, Rauramaa R, Saleheen D, Salomaa V, Sanghera DK, Saramies J, Schwarz PE, Sheu WH, Shuldiner AR, Siegbahn A, Spector TD, Stefansson K, Strachan DP, Tayo BO, Tremoli E, Tuomilehto J, Uusitupa M, van Duijn CM, Vollenweider P, Wallentin L, Wareham NJ, Whitfield JB, Wolffenbuttel BH, Ordovas JM, Boerwinkle E, Palmer CN, Thorsteinsdottir U, Chasman DI, Rotter JI, Franks PW, Ripatti S, Cupples LA, Sandhu MS, Rich SS, Boehnke M, Deloukas P, Kathiresan S, Mohlke KL, Ingelsson E and Abecasis GR. Discovery and refinement of loci associated with lipid levels. *Nat Genet*. 2013;45:1274-83.
14. Franzen O, Ermel R, Cohain A, Akers NK, Di Narzo A, Talukdar HA, Foroughi-Asl H, Giambartolomei C, Fullard JF, Sukhavasi K, Koks S, Gan LM, Giannarelli C, Kovacic JC, Betsholtz C, Losic B, Michoel T, Hao K, Roussos P, Skogsberg J, Ruusalepp A, Schadt EE and Bjorkegren JL. Cardiometabolic risk loci share downstream cis- and trans-gene regulation across tissues and diseases. *Science*. 2016;353:827-30.
15. Li F and Zhang H. Lysosomal Acid Lipase in Lipid Metabolism and Beyond. *Arteriosclerosis, thrombosis, and vascular biology*. 2019;39:850-856.
16. Zhang H. Lysosomal acid lipase and lipid metabolism: new mechanisms, new questions, and new therapies. *Curr Opin Lipidol*. 2018;29:218-223.
17. Porto AF. Lysosomal acid lipase deficiency: diagnosis and treatment of Wolman and Cholesteryl Ester Storage Diseases. *Pediatr Endocrinol Rev*. 2014;12 Suppl 1:125-32.
18. Reiner Ž, Guardamagna O, Nair D, Soran H, Hovingh K, Bertolini S, Jones S, Ćorić M, Calandra S, Hamilton J, Eagleton T and Ros E. Lysosomal acid lipase deficiency--an under-recognized cause of dyslipidaemia and liver dysfunction. *Atherosclerosis*. 2014;235:21-30.
19. Evans TD, Zhang X, Clark RE, Alisio A, Song E, Zhang H, Reilly MP, Stitziel NO and Razani B. Functional Characterization of LIPA (Lysosomal Acid Lipase) Variants Associated With Coronary Artery Disease. *Arterioscler Thromb Vasc Biol*. 2019;39:2480-2491.
20. Susser LI and Rayner KJ. Through the layers: how macrophages drive atherosclerosis across the vessel wall. *J Clin Invest*. 2022;132.

21. Williams JW, Zaitsev K, Kim KW, Ivanov S, Saunders BT, Schrank PR, Kim K, Elvington A, Kim SH, Tucker CG, Wohltmann M, Fife BT, Epelman S, Artyomov MN, Lavine KJ, Zinselmeyer BH, Choi JH and Randolph GJ. Limited proliferation capacity of aortic intima resident macrophages requires monocyte recruitment for atherosclerotic plaque progression. *Nat Immunol*. 2020.
22. Consortium GT. Human genomics. The Genotype-Tissue Expression (GTEx) pilot analysis: multitissue gene regulation in humans. *Science*. 2015;348:648-60.
23. Fernandez JM, de la Torre V, Richardson D, Royo R, Puiggros M, Moncunill V, Fragkogianni S, Clarke L, Consortium B, Flicek P, Rico D, Torrents D, Carrillo de Santa Pau E and Valencia A. The BLUEPRINT Data Analysis Portal. *Cell Syst*. 2016;3:491-495 e5.
24. Chu VT, Weber T, Graf R, Sommermann T, Petsch K, Sack U, Volchkov P, Rajewsky K and Kuhn R. Efficient generation of Rosa26 knock-in mice using CRISPR/Cas9 in C57BL/6 zygotes. *BMC Biotechnol*. 2016;16:4.
25. Hao K, Ermel R, Sukhavasi K, Cheng H, Ma L, Li L, Amadori L, Koplev S, Franzen O, d'Escamard V, Chandel N, Wolhuter K, Bryce NS, Venkata VRM, Miller CL, Ruusalepp A, Schunkert H, Bjorkegren JLM and Kovacic JC. Integrative Prioritization of Causal Genes for Coronary Artery Disease. *Circ Genom Precis Med*. 2022;15:e003365.
26. Giambartolomei C, Vukcevic D, Schadt EE, Franke L, Hingorani AD, Wallace C and Plagnol V. Bayesian test for colocalisation between pairs of genetic association studies using summary statistics. *PLoS Genet*. 2014;10:e1004383.
27. Burgess S, Butterworth A and Thompson SG. Mendelian randomization analysis with multiple genetic variants using summarized data. *Genet Epidemiol*. 2013;37:658-65.
28. Zhu Z, Zhang F, Hu H, Bakshi A, Robinson MR, Powell JE, Montgomery GW, Goddard ME, Wray NR, Visscher PM and Yang J. Integration of summary data from GWAS and eQTL studies predicts complex trait gene targets. *Nat Genet*. 2016;48:481-7.
29. Nurnberg ST, Zhang H, Hand NJ, Bauer RC, Saleheen D, Reilly MP and Rader DJ. From Loci to Biology: Functional Genomics of Genome-Wide Association for Coronary Disease. *Circ Res*. 2016;118:586-606.
30. Turner AW, Hu SS, Mosquera JV, Ma WF, Hodonsky CJ, Wong D, Auguste G, Song Y, Sol-Church K, Farber E, Kundu S, Kundaje A, Lopez NG, Ma L, Ghosh SKB, Onengut-Gumuscu S, Ashley EA, Quertermous T, Finn AV, Leeper NJ, Kovacic JC, Bjorkegren JLM, Zang C and Miller CL. Single-nucleus chromatin accessibility profiling highlights regulatory mechanisms of coronary artery disease risk. *Nat Genet*. 2022;54:804-816.
31. Pham TH, Benner C, Lichtinger M, Schwarzfischer L, Hu Y, Andreesen R, Chen W and Rehli M. Dynamic epigenetic enhancer signatures reveal key transcription factors associated with monocytic differentiation states. *Blood*. 2012;119:e161-71.
32. Nerlov C and Graf T. PU.1 induces myeloid lineage commitment in multipotent hematopoietic progenitors. *Genes Dev*. 1998;12:2403-12.
33. Ahmed N, Etzrodt M, Dettinger P, Kull T, Loeffler D, Hoppe PS, Chavez JS, Zhang Y, Camargo Ortega G, Hilsenbeck O, Nakajima H, Pietras EM and Schroeder T. Blood stem cell PU.1 upregulation is a consequence of differentiation without fast autoregulation. *J Exp Med*. 2022;219.
34. Pham TH, Langmann S, Schwarzfischer L, El Chartouni C, Lichtinger M, Klug M, Krause SW and Rehli M. CCAAT enhancer-binding protein beta regulates constitutive gene expression during late stages of monocyte to macrophage differentiation. *J Biol Chem*. 2007;282:21924-33.
35. Zhu Y and Suh Y. Ultrafine mapping of chromosome conformation at hundred basepair resolution reveals regulatory genome architecture. *bioRxiv*. 2020:743005.
36. Abram CL, Roberge GL, Hu Y and Lowell CA. Comparative analysis of the efficiency and specificity of myeloid-Cre deleting strains using ROSA-EYFP reporter mice. *J Immunol Methods*. 2014;408:89-100.
37. Shi J, Hua L, Harmer D, Li P and Ren G. Cre Driver Mice Targeting Macrophages. *Methods Mol Biol*. 2018;1784:263-275.

38. Gamblin C, Rouault C, Lacombe A, Langa-Vives F, Farabos D, Lamaziere A, Clement K, Gautier EL, Yvan-Charvet L and Dugail I. Lysosomal Acid Lipase Drives Adipocyte Cholesterol Homeostasis and Modulates Lipid Storage in Obesity, Independent of Autophagy. *Diabetes*. 2021;70:76-90.
39. Zagayko A, Kravchenko G, Strelchenko K, Shkapo A and Briukhanova T. Sex and Age Differences in Lipoprotein Metabolism Proatherogenic Changes under the Experimental Metabolic Syndrome in Hamsters. In: K. Gerhard and C. Indumathi, eds. *Lipoproteins* Rijeka: IntechOpen; 2015: Ch. 2.
40. Cai B, Thorp EB, Doran AC, Sansbury BE, Daemen MJ, Dorweiler B, Spite M, Fredman G and Tabas I. MerTK receptor cleavage promotes plaque necrosis and defective resolution in atherosclerosis. *J Clin Invest*. 2017;127:564-568.
41. Robbins CS, Hilgendorf I, Weber GF, Theurl I, Iwamoto Y, Figueiredo JL, Gorbatov R, Sukhova GK, Gerhardt LM, Smyth D, Zavitz CC, Shikatani EA, Parsons M, van Rooijen N, Lin HY, Husain M, Libby P, Nahrendorf M, Weissleder R and Swirski FK. Local proliferation dominates lesional macrophage accumulation in atherosclerosis. *Nat Med*. 2013;19:1166-72.
42. Liu J, Thewke DP, Su YR, Linton MF, Fazio S and Sinensky MS. Reduced macrophage apoptosis is associated with accelerated atherosclerosis in low-density lipoprotein receptor-null mice. *Arterioscler Thromb Vasc Biol*. 2005;25:174-9.
43. Zernecke A, Erhard F, Weinberger T, Schulz C, Ley K, Saliba A-E and Cochain C. Integrated single-cell analysis-based classification of vascular mononuclear phagocytes in mouse and human atherosclerosis. *Cardiovascular Research*. 2022.
44. Zernecke A, Winkels H, Cochain C, Williams JW, Wolf D, Soehnlein O, Robbins CS, Monaco C, Park I, McNamara CA, Binder CJ, Cybulsky MI, Scipione CA, Hedrick CC, Galkina EV, Kyaw T, Ghosheh Y, Dinh HQ and Ley K. Meta-Analysis of Leukocyte Diversity in Atherosclerotic Mouse Aortas. *Circ Res*. 2020;127:402-426.
45. Ensan S, Li A, Besla R, Degousee N, Cosme J, Roufaiel M, Shikatani EA, El-Maklizi M, Williams JW, Robins L, Li C, Lewis B, Yun TJ, Lee JS, Wieghofer P, Khattar R, Farrokhi K, Byrne J, Ouzounian M, Zavitz CC, Levy GA, Bauer CM, Libby P, Husain M, Swirski FK, Cheong C, Prinz M, Hilgendorf I, Randolph GJ, Epelman S, Gramolini AO, Cybulsky MI, Rubin BB and Robbins CS. Self-renewing resident arterial macrophages arise from embryonic CX3CR1(+) precursors and circulating monocytes immediately after birth. *Nat Immunol*. 2016;17:159-68.
46. Cochain C, Vafadarnejad E, Arampatzi P, Pelisek J, Winkels H, Ley K, Wolf D, Saliba AE and Zernecke A. Single-Cell RNA-Seq Reveals the Transcriptional Landscape and Heterogeneity of Aortic Macrophages in Murine Atherosclerosis. *Circ Res*. 2018;122:1661-1674.
47. Fidler TP, Xue C, Yalcinkaya M, Hardaway B, Abramowicz S, Xiao T, Liu W, Thomas DG, Hajebrahimi MA, Pircher J, Silvestre-Roig C, Kotini AG, Luchsinger LL, Wei Y, Westerterp M, Snoeck HW, Papapetrou EP, Schulz C, Massberg S, Soehnlein O, Ebert B, Levine RL, Reilly MP, Libby P, Wang N and Tall AR. The AIM2 inflammasome exacerbates atherosclerosis in clonal haematopoiesis. *Nature*. 2021;592:296-301.
48. Lin JD, Nishi H, Poles J, Niu X, McCauley C, Rahman K, Brown EJ, Yeung ST, Vozhilla N, Weinstock A, Ramsey SA, Fisher EA and Loke P. Single-cell analysis of fate-mapped macrophages reveals heterogeneity, including stem-like properties, during atherosclerosis progression and regression. *JCI Insight*. 2019;4.
49. Endo-Umeda K, Kim E, Thomas DG, Liu W, Dou H, Yalcinkaya M, Abramowicz S, Xiao T, Antonson P, Gustafsson JA, Makishima M, Reilly MP, Wang N and Tall AR. Myeloid LXR (Liver X Receptor) Deficiency Induces Inflammatory Gene Expression in Foamy Macrophages and Accelerates Atherosclerosis. *Arterioscler Thromb Vasc Biol*. 2022;42:719-731.
50. Kim K, Shim D, Lee JS, Zaitsev K, Williams JW, Kim KW, Jang MY, Seok Jang H, Yun TJ, Lee SH, Yoon WK, Prat A, Seidah NG, Choi J, Lee SP, Yoon SH, Nam JW, Seong JK, Oh GT, Randolph GJ, Artyomov MN, Cheong C and Choi JH. Transcriptome Analysis Reveals Nonfoamy Rather Than Foamy Plaque Macrophages Are Proinflammatory in Atherosclerotic Murine Models. *Circ Res*. 2018;123:1127-1142.

51. Potteaux S, Gautier EL, Hutchison SB, van Rooijen N, Rader DJ, Thomas MJ, Sorci-Thomas MG and Randolph GJ. Suppressed monocyte recruitment drives macrophage removal from atherosclerotic plaques of Apoe-/- mice during disease regression. *J Clin Invest*. 2011;121:2025-36.
52. Tajima T, Morita H, Ito K, Yamazaki T, Kubo M, Komuro I and Momozawa Y. Blood lipid-related low-frequency variants in LDLR and PCSK9 are associated with onset age and risk of myocardial infarction in Japanese. *Sci Rep*. 2018;8:8107.
53. Morris GE, Braund PS, Moore JS, Samani NJ, Codd V and Webb TR. Coronary Artery Disease-Associated LIPA Coding Variant rs1051338 Reduces Lysosomal Acid Lipase Levels and Activity in Lysosomes. *Arteriosclerosis, thrombosis, and vascular biology*. 2017;37:1050-1057.
54. Reiner Z, Guardamagna O, Nair D, Soran H, Hovingh K, Bertolini S, Jones S, Coric M, Calandra S, Hamilton J, Eagleton T and Ros E. Lysosomal acid lipase deficiency--an under-recognized cause of dyslipidaemia and liver dysfunction. *Atherosclerosis*. 2014;235:21-30.
55. Frampton JE. Sebelipase Alfa: A Review in Lysosomal Acid Lipase Deficiency. *American journal of cardiovascular drugs : drugs, devices, and other interventions*. 2016;16:461-468.
56. Lopresti MW, Cui W, Abernathy BE, Fredrickson G, Barrow F, Desai AS, Revelo XS and Mashek DG. Hepatic lysosomal acid lipase overexpression worsens hepatic inflammation in mice fed a Western diet. *J Lipid Res*. 2021;62:100133.
57. Spann NJ, Garmire LX, McDonald JG, Myers DS, Milne SB, Shibata N, Reichart D, Fox JN, Shaked I, Heudobler D, Raetz CR, Wang EW, Kelly SL, Sullards MC, Murphy RC, Merrill AH, Jr., Brown HA, Dennis EA, Li AC, Ley K, Tsimikas S, Fahy E, Subramaniam S, Quehenberger O, Russell DW and Glass CK. Regulated accumulation of desmosterol integrates macrophage lipid metabolism and inflammatory responses. *Cell*. 2012;151:138-52.